

Supporting Information

Synthesis, Solid-State, and Solution Characterization of an “In-Cage” Scandium-NOTA Complex

Kelly E. Aldrich,^a Ivan A. Popov,^{a,b} Harrison D. Root,^a Enrique R. Batista,^{a,*} Samuel M. Greer,^a Stosh A. Kozimor,^{a,*} Laura M. Lilley,^a Maksim Y. Livshits,^a Veronika Mocko,^a Michael T. Janicke,^a Benjamin W. Stein,^a Ping Yang^{a,*}

^a Los Alamos National Laboratory, Los Alamos, NM, USA

^b Department of Chemistry, The University of Akron, Akron, Ohio 44325-3601, USA.

Table of Contents

X-Ray Crystallography	3
Crystallographic Details of SOLUTION 1	3
Discussion of the two [Sc(NOTA)(OOCCH ₃)] ¹⁻ Subunits Present Within the Unit Cell.	3
Figure S1. Molecular structure of Sc(NOTA) (top) and [Sc(NOTA)(OOCCH ₃)] ¹⁻ (bottom). Spacefilling models of the structures (based on VanderWalls radii) are shown for comparison obtained from the single crystal X-ray data.....	18
HRMS Analysis	19
Figure S2. Mass Spectrum for Sc(NOTA) (ToF, positive mode).....	19
MS Discussion	19
NMR Spectroscopy	20
General NMR Considerations	20
Figure S3. ¹ H NMR of Na[Sc(NOTA)(OOCCH ₃)] in D ₂ O at 20 °C (pH = 7). Broad peaks indicative of an exchange process.	21
Figure S4. ¹ H NMR of Na[Sc(NOTA)(OOCCH ₃)] in DMSO-d ₆ at 20 °C.....	22
Figure S5. ⁴⁵ Sc NMR of Na[Sc(NOTA)(OOCCH ₃)] in D ₂ O at 20 °C.....	23
Figure S6. ⁴⁵ Sc NMR of Na[Sc-NOTA-OAc] in D ₂ O at 40 °C. Peak fitting was applied.....	24
Figure S7. ⁴⁵ Sc NMR of Na[Sc-NOTA-OAc] in D ₂ O at 80 °C. Peak fitting was applied.....	25
Figure S8. ¹⁷ O NMR spectra of tap water (red) and Na[Sc(NOTA)(OOCCH ₃)] in D ₂ O spiked with H ₂ (¹⁷ O) (green) at 25 °C.....	26
Figure S9. ⁴⁵ Sc NMR of Na[Sc(NOTA)(L)] in dmsO-d ₆ at 20 °C. (where L = ⁻ OOCCH ₃ , DMSO, H ₂ O or a combination of these)	27

Experimental Approximation of Exchange Process Thermodynamics.....	28
Table S4. Van't Hoff plot parameters for VT ⁴⁵ Sc NMR species distributions.	29
Figure S10. Van't Hoff Plot of VT ⁴⁵ Sc NMR species distributions in D ₂ O (ln(K _{eq}) vs. (1/T))	29
IR Spectroscopy	30
Figure S11. IR spectrum of solid Na[Sc(NOTA)(OOCCH ₃)], recorded in transmittance mode.....	30
Discussion of IR.....	30
Computational Details	32
Figure S12. Coordination of water molecule to Na[Sc(NOTA)(OOCCH ₃)] (a) to form Na[Sc(NOTA)(OOCCH ₃)(H ₂ O)] (b).	32
Table S5. Comparison of the bond distances and RMSD values of the [Sc(NOTA)(OOCCH ₃)] ¹⁻ , Na[Sc(NOTA)(OOCCH ₃)] and 2H ₂ O*Na[Sc(NOTA)(OOCCH ₃)] complexes to the experimental XRD structure.	33
Figure S13. Acetate-water substitution in the Na[Sc(NOTA)(OOCCH ₃)] complex (a) to form [Sc(NOTA)(OH ₂)] (b).	33
Figure S14. Acetate-water substitution with two water molecules to the Na[Sc(NOTA)(OOCCH ₃)] complex (a) to form [Sc(NOTA)(OH ₂) ₂] (b).	34
Figure S15. Exchange processes calculated and associated Gibbs free energy change for both the association (a) and exchange mechanisms (b).	36
Discussion of Bulk Water Treatment Using the Cluster Approach	36
Figure S16. Coordination of DMSO molecule to Na[Sc(NOTA)(OOCCH ₃)].	37
Figure S17. Acetate-DMSO substitution with one (a) and two (b) DMSO molecules in the Na[Sc(NOTA)(OOCCH ₃)] complex to form [Sc(NOTA)(DMSO)] (a) and [Sc(NOTA)(DMSO) ₂] (b)	38
Figure S18. Simultaneous addition of DMSO and NaCH ₃ COO to [Sc(NOTA)] (a) to form Na[Sc(NOTA)(CH ₃ COO)(DMSO)] (b).	39
References	39

X-Ray Crystallography

Single crystals of $C_{28}H_{48}N_6Na_3O_{19}Sc_2 \cdot n H_2O$ were grown by layering a solution containing the Na[Sc-NOTA-OAc] complex and byproduct salts in a MeOH/H₂O solution with acetone and chilling the solution to 10 °C for several days. Crystals were clear and colorless and had a plate-like appearance. A suitable crystal was selected and mounted in paratone oil on a nylon loop. The crystal was irradiated on a Bruker D8 Quest diffractometer configured with an CPAD Photon IITM area detector and MoK α ($\lambda = 0.71073 \text{ \AA}$) I μ S 3.0 micro sourceTM. The crystal was kept at 100.0 K during data collection. Using Olex2 [1], the structure was solved with the ShelXT [2] structure solution program using Intrinsic Phasing and refined with the XL [3] refinement package using Least Squares minimization. For Solution 1 below, the SQUEEZE or BYPASS function was applied.

Crystallographic Details of SOLUTION 1

The initial structure solution was determined using the Intrinsic Phasing routine in APEX3 software. Refinement of the solution was performed using Olex2¹ software running SHELX Least Squares refinement.² The “SQUEEZE” function³ was applied to the solution to treat a large number of disordered, outersphere waters occupying the void space of the structure.

Crystal Data for $C_{28}H_{48}N_6Na_3O_{19}Sc_2$ ($M = 931.61 \text{ g/mol}$): monoclinic, space group C2/c (no. 15), $a = 34.9608(7) \text{ \AA}$, $b = 19.7499(4) \text{ \AA}$, $c = 14.5059(3) \text{ \AA}$, $\beta = 107.9050(10)^\circ$, $V = 9530.8(3) \text{ \AA}^3$, $Z = 8$, $T = 100(1) \text{ K}$, $\mu(\text{MoK}\alpha) = 0.382 \text{ mm}^{-1}$, $D_{\text{calc}} = 1.299 \text{ g/cm}^3$, 53239 reflections measured ($4.084^\circ \leq 2\theta \leq 55.834^\circ$), 11371 unique ($R_{\text{int}} = 0.0451$, $R_{\text{sigma}} = 0.0359$) which were used in all calculations. The final R_1 was 0.0427 ($I > 2\sigma(I)$) and wR_2 was 0.0913 (all data).

Discussion of the two [Sc(NOTA)(OOCCH₃)]¹⁻ Subunits Present Within the Unit Cell.

Overlaying the two [Sc(NOTA)(OOCCH₃)]¹⁻ subunits present within the unit cell revealed that the Sc–NOTA and Sc–OOCCH₃ bond distances and angles were nearly identical (Figure 1), and only subtle geometric deviations were apparent. More quantitative evaluation showed slight $<0.0016 \text{ \AA}$ differences between Sc1–O_{NOTA} vs. Sc2–O_{NOTA} bond distances, with the only statistically relevant deviation being between Sc1–O5 and Sc2–O13. The Sc1–N_{NOTA} vs. Sc2–N_{NOTA} distances were similarly similar. Slightly more variation was observed for Sc1–O_{OOCCH₃} vs. Sc2–O_{OOCCH₃} bonds, with deviations of 0.05 and 0.033 \AA between the two analogous sets of acetate oxygen atoms, which slightly exceeded the uncertainty of the crystallographic measurement. We suspected that these small differences between the two symmetry inequivalent [Sc(NOTA)(OOCCH₃)]¹⁻ fragments were the result of subtle variation in the long range electrostatic interactions imparted by the extended structure of the crystalline material (see below), such as the positions of individual H₂O molecules and Na¹⁺ cations.

Table 1 Crystal data and structure refinement for SOLUTION 1.

Identification code	final_BLS_05-13-22
Empirical formula	C ₂₈ H ₇₀ N ₆ Na ₃ O ₃₀ Sc ₂
Formula weight	1129.79
Temperature/K	100.00
Crystal system	monoclinic
Space group	C2/c
a/Å	34.9608(7)
b/Å	19.7499(4)
c/Å	14.5059(3)
α/°	90
β/°	107.9050(10)
γ/°	90
Volume/Å ³	9530.8(3)
Z	8
ρ _{calc} /cm ³	1.575
μ/mm ⁻¹	0.414
F(000)	4760.0
Crystal size/mm ³	0.16 × 0.12 × 0.06
Radiation	MoKα (λ = 0.71073)
2θ range for data collection/°	4.084 to 55.834
Index ranges	-45 ≤ h ≤ 45, -25 ≤ k ≤ 19, -18 ≤ l ≤ 19
Reflections collected	53239
Independent reflections	11371 [R _{int} = 0.0451, R _{sigma} = 0.0359]
Data/restraints/parameters	11371/4/573
Goodness-of-fit on F ²	1.040
Final R indexes [I ≥ 2σ (I)]	R ₁ = 0.0427, wR ₂ = 0.0876
Final R indexes [all data]	R ₁ = 0.0523, wR ₂ = 0.0913
Largest diff. peak/hole / e Å ⁻³	0.40/-0.43

Fractional Atomic Coordinates (×10⁴) and Equivalent Isotropic Displacement Parameters (Å²×10³) for SOLUTION 1. U_{eq} is defined as 1/3 of of the trace of the orthogonalised U_{ij} tensor.

Atom	x	y	z	U(eq)
Sc1	3614.9(2)	8394.9(2)	891.8(2)	10.27(7)
Sc2	3297.0(2)	5816.3(2)	4993.4(3)	11.61(7)
Na1	3066.7(2)	7023.0(3)	1123.7(5)	14.10(15)
Na2	2686.9(2)	8478.9(4)	1164.9(5)	13.32(15)
Na3	2525.6(2)	10222.8(4)	1747.7(5)	15.52(15)
N1	3590.8(5)	8340.0(8)	-766.4(11)	13.7(3)
N2	4296.3(5)	8259.0(8)	948.1(12)	15.1(3)
N3	3868.9(4)	9458.1(8)	544.7(12)	13.8(3)

N4	3760.1(5)	4909.0(8)	5508.4(13)	19.6(4)
N5	3831.8(5)	6270.1(10)	6272.8(13)	25.2(4)
N6	3874.1(5)	6019.6(10)	4424.8(13)	25.9(4)
O1	3052.5(4)	7967.2(6)	120.2(9)	12.4(3)
O2	2580.3(4)	7646.7(6)	-1230.0(9)	14.1(3)
O3	3780.4(4)	7340.1(6)	1161.1(10)	14.9(3)
O4	4256.7(5)	6599.9(7)	1925.9(13)	32.7(4)
O5	3218.1(4)	9196.0(6)	1033.2(9)	14.3(3)
O6	3173.6(4)	10227.8(7)	1619.8(11)	23.4(3)
O7	3327.2(4)	8021.3(6)	2089.5(9)	14.1(3)
O8	3893.7(4)	8583.3(7)	2459.5(10)	16.8(3)
O9	2943.5(4)	4920.0(6)	4842.6(9)	14.0(3)
O10	2890.3(4)	3797.3(6)	4932.3(10)	18.2(3)
O11	3098.1(4)	5934.9(7)	6252.8(10)	16.1(3)
O12	3181.1(5)	6405.6(8)	7707.8(11)	25.4(3)
O13	3151.3(4)	5623.5(6)	3460.0(10)	15.8(3)
O14	3143.9(4)	6114.2(7)	2077.0(10)	20.4(3)
O15	2649.0(4)	6232.8(6)	4303.1(10)	16.6(3)
O16	3180.3(4)	6881.7(7)	4618.5(11)	21.0(3)
O17	2639.2(4)	10586.9(8)	3391.4(11)	22.7(3)
O18	2538.5(4)	9097.0(7)	2338.7(10)	18.2(3)
O19	2793.1(5)	9253.1(9)	4354.9(11)	32.3(4)
C1	2915.8(5)	7873.2(8)	-806.5(13)	11.5(3)
C2	3196.3(5)	8058.7(10)	-1376.1(14)	16.7(4)
C3	3918.2(6)	7849.7(10)	-738.8(14)	17.7(4)
C4	4321.0(6)	8060.7(10)	-33.4(14)	17.8(4)
C5	4145.7(6)	7162.7(10)	1570.3(15)	18.4(4)
C6	4457.9(5)	7712.1(10)	1655.4(15)	16.9(4)
C7	4519.7(6)	8898.3(10)	1299.0(15)	17.5(4)
C8	4310.3(5)	9488.1(10)	681.4(15)	16.6(4)
C9	3347.9(6)	9796.2(9)	1280.9(14)	15.4(4)
C10	3758.1(5)	9961.3(9)	1172.4(15)	16.7(4)
C11	3632.6(6)	9588.3(9)	-485.2(14)	16.6(4)
C12	3674.4(6)	9017.9(9)	-1141.9(14)	16.7(4)
C13	3612.5(6)	8303.5(9)	2721.2(14)	15.3(4)
C14	3621.2(7)	8336.7(11)	3758.3(15)	24.6(4)
C15	3089.3(6)	4326.6(9)	5020.5(13)	14.2(4)
C16	3540.1(6)	4257.9(9)	5320.9(15)	18.7(4)
C19	3282.3(6)	6312.0(10)	6975.1(14)	17.9(4)
C20	3644.3(6)	6681.2(11)	6866.1(16)	25.5(5)
C23	3300.9(6)	6002.5(9)	2948.6(14)	16.3(4)
C24	3698.6(6)	6340.8(12)	3470.0(15)	24.5(5)

C27	2799.2(6)	6810.9(9)	4277.3(14)	16.1(4)
C28	2543.4(6)	7404.3(10)	3827.6(15)	21.6(4)
C17A	3879.7(8)	5047.4(13)	6608.6(18)	17.0(5)
C18A	4070.1(8)	5746.3(15)	6850(2)	18.1(6)
C21A	4065.0(9)	6760.6(15)	5817(2)	18.0(5)
C22A	4207.2(9)	6394.4(17)	5064(2)	19.9(6)
C25A	4025.7(8)	5296.0(15)	4268(2)	17.6(5)
C26A	4113.3(8)	4891.4(13)	5190(2)	18.9(5)
C17B	4106(2)	4978(4)	6315(6)	18.0(5)
C18B	3985(3)	5490(5)	6911(7)	18.0(5)
C21B	4211(3)	6482(5)	6190(6)	19.6(16)
C22B	4081(3)	6716(5)	5144(6)	17.5(16)
C25B	4125(3)	5591(5)	4431(7)	18.0(5)
C26B	3939(2)	4908(4)	4538(6)	18.0(5)

Anisotropic Displacement Parameters ($\text{\AA}^2 \times 10^3$) for SOLUTION 1. The Anisotropic displacement factor exponent takes the form: $-2\pi^2[h^2a^{*2}U_{11}+2hka^*b^*U_{12}+\dots]$.

Atom	U_{11}	U_{22}	U_{33}	U_{23}	U_{13}	U_{12}
Sc1	9.48(15)	10.01(15)	11.03(16)	-1.31(12)	2.72(12)	-1.65(12)
Sc2	12.46(15)	10.31(15)	12.09(17)	0.45(13)	3.80(13)	-0.37(13)
Na1	17.0(4)	11.0(3)	13.6(4)	0.0(3)	3.5(3)	-1.7(3)
Na2	12.6(3)	12.2(3)	14.9(4)	-1.9(3)	3.8(3)	-0.3(3)
Na3	16.4(4)	14.7(3)	15.0(4)	-1.2(3)	4.2(3)	0.3(3)
N1	14.4(7)	14.3(7)	13.3(8)	-1.8(6)	5.5(6)	-4.2(6)
N2	14.4(7)	13.8(7)	16.2(8)	-0.4(6)	3.6(6)	-1.2(6)
N3	12.7(7)	12.6(7)	16.6(8)	-1.3(6)	5.3(6)	-1.9(6)
N4	15.4(8)	13.9(8)	26.3(9)	2.8(7)	1.6(7)	0.1(6)
N5	18.4(8)	36.3(10)	24.0(10)	-15.5(8)	11.2(8)	-9.7(8)
N6	17.7(8)	43.6(11)	15.1(9)	5.8(8)	3.3(7)	-7.6(8)
O1	12.6(6)	12.9(6)	11.2(6)	-0.6(5)	2.8(5)	-1.8(5)
O2	13.2(6)	15.6(6)	12.5(6)	-1.0(5)	2.3(5)	-2.7(5)
O3	11.7(6)	13.2(6)	18.6(7)	-1.5(5)	3.0(5)	-0.8(5)
O4	21.3(7)	16.4(7)	51.1(11)	10.3(7)	-2.5(7)	1.2(6)
O5	13.7(6)	11.2(6)	18.0(7)	-2.8(5)	5.0(5)	-1.7(5)
O6	22.2(7)	17.9(7)	32.7(9)	-11.5(6)	12.5(7)	-2.7(6)
O7	14.3(6)	13.5(6)	13.1(6)	-1.9(5)	2.1(5)	-1.1(5)
O8	13.9(6)	19.8(7)	15.9(7)	-3.0(5)	3.7(5)	-3.4(5)
O9	16.1(6)	10.2(6)	13.9(6)	2.2(5)	1.9(5)	-0.5(5)
O10	21.5(7)	12.3(6)	15.8(7)	2.9(5)	-1.7(6)	-4.0(5)
O11	17.7(6)	17.0(6)	14.3(7)	-1.3(5)	5.8(5)	-1.5(5)

O12	29.4(8)	30.6(8)	19.5(8)	-9.6(6)	12.5(6)	-6.5(7)
O13	19.7(6)	15.1(6)	13.7(7)	1.4(5)	6.4(5)	-2.4(5)
O14	25.7(7)	20.4(7)	14.5(7)	5.0(6)	5.2(6)	-2.0(6)
O15	17.7(6)	12.3(6)	19.7(7)	0.0(5)	5.5(6)	0.0(5)
O16	17.4(7)	14.1(6)	28.6(8)	3.6(6)	2.8(6)	-0.6(5)
O17	21.1(7)	24.0(8)	20.0(8)	-3.0(6)	1.9(6)	1.9(6)
O18	21.3(7)	19.0(7)	15.6(7)	-2.3(6)	7.4(6)	-0.4(6)
O19	41.0(10)	39.8(10)	18.3(8)	-4.3(7)	12.4(7)	-19.1(8)
C1	13.3(8)	7.0(7)	13.7(9)	0.1(6)	3.6(7)	0.1(6)
C2	15.2(9)	22.5(10)	12.0(9)	-2.1(7)	3.7(7)	-5.2(8)
C3	19.8(9)	18.1(9)	16.7(9)	-2.4(8)	8.0(8)	-0.4(8)
C4	14.9(9)	21.0(10)	19.1(10)	-2.0(8)	7.3(8)	2.0(7)
C5	16.8(9)	16.6(9)	20.5(10)	-1.5(8)	3.7(8)	0.0(7)
C6	12.7(8)	16.6(9)	19.4(10)	1.0(7)	2.1(8)	1.3(7)
C7	12.4(8)	18.5(9)	20.9(10)	-3.5(8)	3.9(8)	-4.8(7)
C8	11.9(8)	17.4(9)	20.7(10)	-0.2(8)	5.5(8)	-3.4(7)
C9	16.7(9)	13.9(8)	14.6(9)	-2.7(7)	3.4(7)	-0.8(7)
C10	14.9(8)	13.3(9)	21.9(10)	-4.9(7)	5.6(8)	-3.0(7)
C11	16.4(9)	15.2(9)	17.8(10)	2.0(7)	4.7(8)	-1.1(7)
C12	17.8(9)	18.3(9)	14.6(9)	1.9(7)	5.9(8)	-5.2(7)
C13	17.7(9)	13.6(8)	14.0(9)	-1.6(7)	4.0(7)	1.2(7)
C14	29.2(11)	28.2(11)	15.9(10)	-5.9(8)	6.2(9)	-8.3(9)
C15	19.6(9)	15.0(9)	6.3(8)	1.7(7)	1.5(7)	0.2(7)
C16	18.6(9)	12.3(9)	24.3(11)	0.9(8)	5.3(8)	0.6(7)
C19	20.6(9)	15.4(9)	17.8(10)	-1.4(7)	6.1(8)	1.9(8)
C20	26.4(11)	29.4(11)	24.9(11)	-15.1(9)	14.2(9)	-9.0(9)
C23	20.1(9)	14.4(9)	15.4(9)	0.8(7)	6.8(8)	1.0(7)
C24	25.1(10)	33.1(12)	16.0(10)	2.7(9)	7.3(9)	-11.7(9)
C27	20.1(9)	13.2(8)	14.5(9)	-0.2(7)	4.4(8)	1.6(7)
C28	25.0(10)	14.4(9)	22.9(11)	1.0(8)	3.8(9)	3.5(8)
C17A	19.1(12)	16.4(12)	13.3(12)	1.3(10)	1.7(10)	-0.2(10)
C18A	12.9(12)	23.4(14)	15.6(13)	-4.1(11)	0.8(10)	-2.0(11)
C21A	16.8(11)	17.6(12)	19.3(13)	-0.9(10)	4.9(10)	-4.3(9)
C22A	21.1(14)	19.6(15)	21.8(15)	-3.1(12)	10.4(12)	-5.9(12)
C25A	16.3(13)	18.6(13)	19.8(14)	-4.6(11)	8.5(11)	1.0(11)
C26A	16.2(12)	17.9(12)	23.5(15)	-3.6(11)	7.3(11)	1.8(10)
C17B	16.8(11)	17.6(12)	19.3(13)	-0.9(10)	4.9(10)	-4.3(9)
C18B	16.8(11)	17.6(12)	19.3(13)	-0.9(10)	4.9(10)	-4.3(9)
C21B	21(4)	20(4)	17(4)	-3(3)	6(3)	-5(3)
C22B	20(4)	16(4)	14(4)	-5(3)	2(3)	-14(3)
C25B	16.8(11)	17.6(12)	19.3(13)	-0.9(10)	4.9(10)	-4.3(9)
C26B	16.8(11)	17.6(12)	19.3(13)	-0.9(10)	4.9(10)	-4.3(9)

Table 4 Bond Lengths for SOLUTION 1.

Atom	Atom	Length/Å	Atom	Atom	Length/Å
Sc1	N1	2.3834(16)	N4	C26A	1.446(3)
Sc1	N2	2.3738(16)	N4	C17B	1.407(8)
Sc1	N3	2.3932(15)	N4	C26B	1.707(8)
Sc1	O1	2.1163(13)	N5	C20	1.475(3)
Sc1	O3	2.1652(13)	N5	C18A	1.427(3)
Sc1	O5	2.1551(13)	N5	C21A	1.540(3)
Sc1	O7	2.3765(13)	N5	C18B	1.792(10)
Sc1	O8	2.2129(14)	N5	C21B	1.431(8)
Sc2	N4	2.3762(16)	N6	C24	1.475(3)
Sc2	N5	2.3684(18)	N6	C22A	1.449(3)
Sc2	N6	2.4364(17)	N6	C25A	1.565(3)
Sc2	O9	2.1314(13)	N6	C22B	1.743(8)
Sc2	O11	2.1580(13)	N6	C25B	1.219(9)
Sc2	O13	2.1576(14)	O1	C1	1.294(2)
Sc2	O15	2.3275(13)	O2	C1	1.229(2)
Sc2	O16	2.1802(14)	O3	C5	1.281(2)
Na1	O1	2.3569(14)	O4	C5	1.237(2)
Na1	O2 ¹	2.4041(14)	O5	C9	1.281(2)
Na1	O3	2.5567(14)	O6	C9	1.234(2)
Na1	O7	2.4281(14)	O7	C13	1.258(2)
Na1	O10 ²	2.3099(15)	O8	C13	1.283(2)
Na1	O14	2.2309(15)	O9	C15	1.272(2)
Na1	C15 ²	3.1223(19)	O10	C15	1.240(2)
Na2	O1	2.4782(14)	O11	C19	1.285(2)
Na2	O2 ¹	2.4244(14)	O12	C19	1.233(2)
Na2	O5	2.3894(14)	O13	C23	1.274(2)
Na2	O7	2.4042(14)	O14	C23	1.234(2)
Na2	O10 ³	2.2422(15)	O15	C27	1.262(2)
Na2	O18	2.2808(15)	O16	C27	1.278(2)
Na3	O6	2.3294(15)	C1	C2	1.509(2)
Na3	O9 ³	2.4583(15)	C3	C4	1.522(3)
Na3	O13 ³	2.4245(15)	C5	C6	1.517(3)
Na3	O15 ³	2.4704(15)	C7	C8	1.514(3)
Na3	O17	2.4036(17)	C9	C10	1.525(3)
Na3	O18	2.3785(16)	C11	C12	1.511(3)
N1	C2	1.498(2)	C13	C14	1.497(3)
N1	C3	1.490(2)	C15	C16	1.507(3)
N1	C12	1.508(2)	C19	C20	1.510(3)

N2	C4	1.504(2)	C23	C24	1.518(3)
N2	C6	1.477(2)	C27	C28	1.497(3)
N2	C7	1.490(2)	C17A	C18A	1.526(4)
N3	C8	1.495(2)	C21A	C22A	1.516(4)
N3	C10	1.478(2)	C25A	C26A	1.507(4)
N3	C11	1.491(2)	C17B	C18B	1.475(12)
N4	C16	1.480(2)	C21B	C22B	1.515(12)
N4	C17A	1.545(3)	C25B	C26B	1.525(11)

¹/2-X,³/2-Y,-Z; ²+X,1-Y,-1/2+Z; ³/2-X,1/2+Y,1/2-Z

Bond Angles for SOLUTION 1.

Atom	Atom	Atom	Angle/°	Atom	Atom	Atom	Angle/°
N1	Sc1	N3	74.20(5)	C11	N3	C8	110.96(14)
N2	Sc1	N1	75.71(5)	C16	N4	Sc2	109.40(11)
N2	Sc1	N3	70.91(5)	C16	N4	C17A	107.69(16)
N2	Sc1	O7	125.84(5)	C16	N4	C26B	98.6(3)
O1	Sc1	N1	73.10(5)	C17A	N4	Sc2	97.65(12)
O1	Sc1	N2	137.09(5)	C26A	N4	Sc2	118.94(14)
O1	Sc1	N3	125.69(5)	C26A	N4	C16	111.53(17)
O1	Sc1	O3	82.23(5)	C26A	N4	C17A	110.37(18)
O1	Sc1	O5	79.79(5)	C17B	N4	Sc2	121.1(3)
O1	Sc1	O7	74.31(5)	C17B	N4	C16	120.2(3)
O1	Sc1	O8	130.90(5)	C17B	N4	C26B	104.3(4)
O3	Sc1	N1	93.60(5)	C26B	N4	Sc2	97.4(3)
O3	Sc1	N2	71.06(5)	C20	N5	Sc2	106.28(12)
O3	Sc1	N3	141.85(5)	C20	N5	C21A	107.03(18)
O3	Sc1	O7	73.69(5)	C20	N5	C18B	106.7(3)
O3	Sc1	O8	88.14(5)	C18A	N5	Sc2	111.30(15)
O5	Sc1	N1	107.78(5)	C18A	N5	C20	109.90(19)
O5	Sc1	N2	138.44(5)	C18A	N5	C21A	114.7(2)
O5	Sc1	N3	70.56(5)	C21A	N5	Sc2	107.25(15)
O5	Sc1	O3	146.44(5)	C18B	N5	Sc2	96.8(3)
O5	Sc1	O7	74.27(5)	C21B	N5	Sc2	125.0(4)
O5	Sc1	O8	82.63(5)	C21B	N5	C20	118.5(4)
O7	Sc1	N1	146.32(5)	C21B	N5	C18B	99.1(5)
O7	Sc1	N3	133.95(5)	C24	N6	Sc2	103.89(12)
O8	Sc1	N1	155.85(5)	C24	N6	C25A	108.52(18)
O8	Sc1	N2	82.15(5)	C24	N6	C22B	101.5(3)
O8	Sc1	N3	89.65(5)	C22A	N6	Sc2	116.97(16)
O8	Sc1	O7	56.82(5)	C22A	N6	C24	113.70(19)
N4	Sc2	N6	71.08(6)	C22A	N6	C25A	108.6(2)

N5	Sc2	N4	75.03(6)	C25A N6	Sc2	104.57(14)
N5	Sc2	N6	70.52(6)	C22B N6	Sc2	99.3(3)
O9	Sc2	N4	73.95(5)	C25B N6	Sc2	123.6(4)
O9	Sc2	N5	133.46(6)	C25B N6	C24	113.4(5)
O9	Sc2	N6	128.07(6)	C25B N6	C22B	112.3(6)
O9	Sc2	O11	81.34(5)	Sc1 O1	Na1	98.59(5)
O9	Sc2	O13	78.58(5)	Sc1 O1	Na2	94.81(5)
O9	Sc2	O15	78.01(5)	Na1 O1	Na2	82.06(5)
O9	Sc2	O16	135.87(5)	C1 O1	Sc1	126.36(11)
O11	Sc2	N4	100.46(6)	C1 O1	Na1	117.31(11)
O11	Sc2	N5	71.20(5)	C1 O1	Na2	126.77(11)
O11	Sc2	N6	141.69(6)	Na1 ¹ O2	Na2 ¹	82.24(4)
O11	Sc2	O15	78.54(5)	C1 O2	Na1 ¹	129.90(12)
O11	Sc2	O16	91.26(5)	C1 O2	Na2 ¹	129.37(12)
O13	Sc2	N4	96.50(6)	Sc1 O3	Na1	91.55(5)
O13	Sc2	N5	138.93(6)	C5 O3	Sc1	121.32(12)
O13	Sc2	N6	68.76(6)	C5 O3	Na1	140.40(12)
O13	Sc2	O11	148.91(5)	Sc1 O5	Na2	96.38(5)
O13	Sc2	O15	74.26(5)	C9 O5	Sc1	121.55(11)
O13	Sc2	O16	86.92(5)	C9 O5	Na2	138.02(12)
O15	Sc2	N4	151.73(5)	C9 O6	Na3	129.80(13)
O15	Sc2	N5	129.26(6)	Sc1 O7	Na1	89.90(5)
O15	Sc2	N6	126.44(6)	Sc1 O7	Na2	90.36(5)
O16	Sc2	N4	149.70(6)	Na2 O7	Na1	82.16(5)
O16	Sc2	N5	82.66(6)	C13 O7	Sc1	88.64(11)
O16	Sc2	N6	82.38(6)	C13 O7	Na1	148.50(12)
O16	Sc2	O15	57.91(5)	C13 O7	Na2	129.31(12)
O1	Na1	O2 ¹	89.04(5)	C13 O8	Sc1	95.52(11)
O1	Na1	O3	69.78(5)	Sc2 O9	Na3 ⁴	95.32(5)
O1	Na1	O7	69.31(5)	C15 O9	Sc2	124.10(12)
O1	Na1	C15 ²	110.98(5)	C15 O9	Na3 ⁴	121.63(11)
O2 ¹	Na1	O3	149.69(5)	Na2 ⁴ O10	Na1 ⁵	108.02(6)
O2 ¹	Na1	O7	86.33(5)	C15 O10	Na1 ⁵	120.12(12)
O2 ¹	Na1	C15 ²	115.92(5)	C15 O10	Na2 ⁴	131.57(12)
O3	Na1	C15 ²	92.39(5)	C19 O11	Sc2	122.80(12)
O7	Na1	O3	66.32(4)	Sc2 O13	Na3 ⁴	95.62(5)
O7	Na1	C15 ²	157.64(5)	C23 O13	Sc2	119.18(12)
O10 ²	Na1	O1	98.21(5)	C23 O13	Na3 ⁴	132.78(12)
O10 ²	Na1	O2 ¹	101.44(5)	C23 O14	Na1	135.25(13)
O10 ²	Na1	O3	102.82(5)	Sc2 O15	Na3 ⁴	90.19(5)
O10 ²	Na1	O7	165.39(6)	C27 O15	Sc2	88.49(11)
O10 ²	Na1	C15 ²	20.09(5)	C27 O15	Na3 ⁴	137.58(12)

O14	Na1	O1	174.27(6)	C27	O16	Sc2	94.82(11)
O14	Na1	O2 ¹	96.63(5)	Na2	O18	Na3	102.40(6)
O14	Na1	O3	104.64(5)	O1	C1	C2	116.07(15)
O14	Na1	O7	110.07(6)	O2	C1	O1	124.20(16)
O14	Na1	O10 ²	81.55(5)	O2	C1	C2	119.73(16)
O14	Na1	C15 ²	67.27(5)	N1	C2	C1	113.72(15)
O2 ¹	Na2	O1	85.83(5)	N1	C3	C4	112.61(15)
O5	Na2	O1	68.48(5)	N2	C4	C3	113.39(15)
O5	Na2	O2 ¹	149.87(5)	O3	C5	C6	115.61(16)
O5	Na2	O7	69.77(5)	O4	C5	O3	125.41(18)
O7	Na2	O1	67.74(5)	O4	C5	C6	118.91(17)
O7	Na2	O2 ¹	86.41(5)	N2	C6	C5	110.76(15)
O10 ³	Na2	O1	101.60(5)	N2	C7	C8	110.03(15)
O10 ³	Na2	O2 ¹	90.65(5)	N3	C8	C7	109.86(15)
O10 ³	Na2	O5	109.21(6)	O5	C9	C10	115.62(16)
O10 ³	Na2	O7	169.10(6)	O6	C9	O5	125.11(17)
O10 ³	Na2	O18	91.03(6)	O6	C9	C10	119.23(16)
O18	Na2	O1	162.40(6)	N3	C10	C9	110.65(15)
O18	Na2	O2 ¹	106.43(5)	N3	C11	C12	111.84(15)
O18	Na2	O5	95.93(5)	N1	C12	C11	111.55(15)
O18	Na2	O7	99.86(5)	O7	C13	O8	118.90(17)
O6	Na3	O9 ³	108.10(6)	O7	C13	C14	121.21(17)
O6	Na3	O13 ³	157.63(6)	O8	C13	C14	119.86(17)
O6	Na3	O15 ³	90.53(5)	O9	C15	Na1 ⁵	144.94(13)
O6	Na3	O17	102.10(6)	O9	C15	C16	117.38(16)
O6	Na3	O18	96.98(6)	O10	C15	Na1 ⁵	39.79(9)
O9 ³	Na3	O15 ³	69.54(5)	O10	C15	O9	125.34(17)
O13 ³	Na3	O9 ³	67.59(5)	O10	C15	C16	117.23(16)
O13 ³	Na3	O15 ³	67.25(5)	C16	C15	Na1 ⁵	87.93(11)
O17	Na3	O9 ³	149.64(6)	N4	C16	C15	114.41(15)
O17	Na3	O13 ³	83.28(5)	O11	C19	C20	114.87(17)
O17	Na3	O15 ³	107.74(6)	O12	C19	O11	125.78(18)
O18	Na3	O9 ³	92.52(5)	O12	C19	C20	119.31(18)
O18	Na3	O13 ³	105.05(5)	N5	C20	C19	109.39(16)
O18	Na3	O15 ³	161.98(6)	O13	C23	C24	116.46(17)
O18	Na3	O17	86.74(6)	O14	C23	O13	124.67(18)
C2	N1	Sc1	110.69(11)	O14	C23	C24	118.86(17)
C2	N1	C12	111.20(15)	N6	C24	C23	109.36(16)
C3	N1	Sc1	102.35(11)	O15	C27	O16	118.75(17)
C3	N1	C2	109.58(14)	O15	C27	C28	121.53(17)
C3	N1	C12	110.74(14)	O16	C27	C28	119.68(17)
C12	N1	Sc1	111.94(11)	C18A	C17A	N4	111.0(2)

C4	N2	Sc1	110.24(11)	N5	C18AC17A	112.7(2)
C6	N2	Sc1	105.79(11)	C22AC21AN5	110.1(2)	
C6	N2	C4	110.24(15)	N6	C22AC21A	109.2(2)
C6	N2	C7	109.51(15)	C26AC25AN6	109.9(2)	
C7	N2	Sc1	109.34(11)	N4	C26AC25A	108.1(2)
C7	N2	C4	111.56(15)	N4	C17BC18B	103.0(6)
C8	N3	Sc1	116.19(11)	C17BC18BN5	112.3(7)	
C10	N3	Sc1	106.01(11)	N5	C21BC22B	99.9(7)
C10	N3	C8	110.30(14)	C21BC22BN6	107.5(6)	
C10	N3	C11	109.40(15)	N6	C25BC26B	106.5(7)
C11	N3	Sc1	103.59(10)	C25BC26BN4	111.1(6)	

¹1/2-X,3/2-Y,-Z; ²+X,1-Y,-1/2+Z; ³1/2-X,1/2+Y,1/2-Z; ⁴1/2-X,-1/2+Y,1/2-Z; ⁵+X,1-Y,1/2+Z

Torsion Angles for SOLUTION 1.

A	B	C	D	Angle/°	A	B	C	D	Angle/°
Sc1	N1	C2	C1	-0.68(19)	Na3 ³	O15	C27	C28	87.6(2)
Sc1	N1	C3	C4	-55.46(16)	N1	C3	C4	N2	48.3(2)
Sc1	N1	C12	C11	-16.53(18)	N2	C7	C8	N3	46.7(2)
Sc1	N2	C4	C3	-12.54(19)	N3	C11	C12	N1	51.1(2)
Sc1	N2	C6	C5	38.12(17)	N4	C17AC18AN5			51.2(3)
Sc1	N2	C7	C8	-54.21(17)	N4	C17BC18BN5			-58.2(7)
Sc1	N3	C8	C7	-17.17(19)	N5	C21AC22AN6			48.6(3)
Sc1	N3	C10	C9	-35.94(17)	N5	C21BC22BN6			-61.0(7)
Sc1	N3	C11	C12	-56.74(16)	N6	C25AC26AN4			53.2(3)
Sc1	O1	C1	O2	177.05(13)	N6	C25BC26BN4			-52.6(8)
Sc1	O1	C1	C2	3.1(2)	O1	C1	C2	N1	-1.2(2)
Sc1	O3	C5	O4	164.55(17)	O2	C1	C2	N1	178.89(16)
Sc1	O3	C5	C6	-12.3(2)	O3	C5	C6	N2	-20.6(2)
Sc1	O5	C9	O6	159.96(16)	O4	C5	C6	N2	162.26(19)
Sc1	O5	C9	C10	17.7(2)	O5	C9	C10	N3	16.2(2)
Sc1	O7	C13	O8	-3.51(17)	O6	C9	C10	N3	166.06(17)
Sc1	O7	C13	C14	174.46(17)	O9	C15	C16	N4	8.5(3)
Sc1	O8	C13	O7	3.78(18)	O10	C15	C16	N4	174.13(17)
Sc1	O8	C13	C14	174.21(16)	O11	C19	C20	N5	-31.1(3)
Sc2	N4	C16	C15	-9.5(2)	O12	C19	C20	N5	151.04(19)
Sc2	N4	C17AC18A		-60.86(19)	O13	C23	C24	N6	13.7(3)
Sc2	N4	C26AC25A		-23.6(3)	O14	C23	C24	N6	167.00(18)

Sc2 N4 C17B C18B	27.5(7)	C2 N1 C3 C4	172.95(15)
Sc2 N4 C26B C25B	59.3(6)	C2 N1 C12 C11	107.86(17)
Sc2 N5 C20 C19	41.4(2)	C3 N1 C2 C1	111.47(17)
Sc2 N5 C18A C17A	-10.0(3)	C3 N1 C12 C11	130.05(16)
Sc2 N5 C21A C22A	-56.7(3)	C4 N2 C6 C5	-81.04(18)
Sc2 N5 C18B C17B	59.7(6)	C4 N2 C7 C8	67.98(19)
Sc2 N5 C21B C22B	31.3(8)	C6 N2 C4 C3	103.88(18)
Sc2 N6 C24 C23	-39.14(19)	C6 N2 C7 C8	169.70(15)
Sc2 N6 C22A C21A	-17.4(3)	C7 N2 C4 C3	134.21(17)
Sc2 N6 C25A C26A	-55.9(2)	C7 N2 C6 C5	155.85(15)
Sc2 N6 C22B C21B	64.1(7)	C8 N3 C10 C9	162.51(15)
Sc2 N6 C25B C26B	17.4(9)	C8 N3 C11 C12	68.63(19)
Sc2 O9 C15 Na1 ¹	129.52(17)	C10 N3 C8 C7	103.48(18)
Sc2 O9 C15 O10	179.48(14)	C10 N3 C11 C12	169.45(15)
Sc2 O9 C15 C16	-2.3(2)	C11 N3 C8 C7	135.13(16)
Sc2 O11 C19 O12	179.16(16)	C11 N3 C10 C9	75.17(19)
Sc2 O11 C19 C20	1.4(2)	C12 N1 C2 C1	125.76(16)
Sc2 O13 C23 O14	152.57(16)	C12 N1 C3 C4	64.0(2)
Sc2 O13 C23 C24	26.7(2)	C16 N4 C17A C18A	174.09(18)
Sc2 O15 C27 O16	-1.61(18)	C16 N4 C26A C25A	105.2(2)
Sc2 O15 C27 C28	176.24(17)	C16 N4 C17B C18B	-115.5(5)
Sc2 O16 C27 O15	1.73(19)	C16 N4 C26B C25B	170.3(6)
Sc2 O16 C27 C28	176.16(16)	C20 N5 C18A C17A	107.4(2)
Na1 O1 C1 O2	56.9(2)	C20 N5 C21A C22A	-170.4(2)
Na1 O1 C1 C2	123.01(14)	C20 N5 C18B C17B	169.0(6)
Na1 ² O2 C1 O1	49.5(2)	C20 N5 C21B C22B	-109.1(6)
Na1 ² O2 C1 C2	130.62(15)	C24 N6 C22A C21A	103.8(3)
Na1 O3 C5 O4	22.8(3)	C24 N6 C25A C26A	166.31(19)
Na1 O3 C5 C6	154.08(14)	C24 N6 C22B C21B	170.4(6)
Na1 O7 C13 O8	84.1(3)	C24 N6 C25B C26B	-109.6(6)
Na1 O7 C13 C14	-98.0(3)	C17A N4 C16 C15	95.6(2)

Na1 ¹ O10C15	O9	135.77(16)	C17AN4	C26AC25A	-135.2(2)
Na1 ¹ O10C15	C16	47.1(2)	C18AN5	C20 C19	-79.1(2)
Na1 ¹ O14C23	O13	138.94(16)	C18AN5	C21AC22A	67.4(3)
Na1 ¹ O14C23	C24	-40.3(3)	C21AN5	C20 C19	155.8(2)
Na1 ¹ C15C16	N4	146.18(15)	C21AN5	C18AC17A	-132.0(2)
Na2 ² O1 C1	O2	-44.2(2)	C22AN6	C24 C23	-167.4(2)
Na2 ² O1 C1	C2	135.92(13)	C22AN6	C25AC26A	69.7(3)
Na2 ² O2 C1	O1	-67.8(2)	C25AN6	C24 C23	71.7(2)
Na2 ² O2 C1	C2	112.10(17)	C25AN6	C22AC21A	-135.3(2)
Na2 ² O5 C9	O6	-8.6(3)	C26AN4	C16 C15	143.19(19)
Na2 ² O5 C9	C10	169.02(13)	C26AN4	C17AC18A	63.9(2)
Na2 ² O7 C13	O8	-92.85(19)	C17BN4	C16 C15	137.4(4)
Na2 ² O7 C13	C14	85.1(2)	C17BN4	C26BC25B	-65.5(7)
Na2 ³ O10C15	Na1 ¹	172.9(2)	C18BN5	C20 C19	-61.0(4)
Na2 ³ O10C15	O9	37.2(3)	C18BN5	C21BC22B	136.2(6)
Na2 ³ O10C15	C16	140.02(15)	C21BN5	C20 C19	-171.5(5)
Na3 ³ O6 C9	O5	-9.8(3)	C21BN5	C18BC17B	-67.5(7)
Na3 ³ O6 C9	C10	172.61(13)	C22BN6	C24 C23	-141.8(4)
Na3 ³ O9 C15	Na1 ¹	107.21(19)	C22BN6	C25BC26B	136.1(6)
Na3 ³ O9 C15	O10	-56.2(2)	C25BN6	C24 C23	97.6(5)
Na3 ³ O9 C15	C16	120.96(15)	C25BN6	C22BC21B	-68.2(8)
Na3 ³ O13C23	O14	-20.5(3)	C26BN4	C16 C15	-110.5(3)
Na3 ³ O13C23	C24	158.73(14)	C26BN4	C17BC18B	135.4(6)
Na3 ³ O15C27	O16	-90.2(2)			

¹X,1-Y,1/2+Z; ²1/2-X,3/2-Y,-Z; ³1/2-X,-1/2+Y,1/2-Z

Hydrogen Atom Coordinates ($\text{\AA}\times 10^4$) and Isotropic Displacement Parameters ($\text{\AA}^2\times 10^3$) for SOLUTION 1.

Atom	x	y	z	U(eq)
H2A	3247.27	7650.54	-1716.9	20
H2B	3062.58	8397.66	-1873.65	20
H3A	3945.35	7809.21	-1396.09	21
H3B	3843.94	7398.9	-548.96	21
H4A	4513.05	7680.7	44.27	21
H4B	4427.75	8447.87	-312.08	21
H6A	4539.31	7901.45	2319.39	20
H6B	4699.21	7514.45	1538.78	20
H7A	4797.7	8858.77	1267.43	21

H7B	4533.77	8977.97	1982.45	21
H8A	4421.45	9919.49	999.94	20
H8B	4357.63	9470.51	43.16	20
H10A	3750.95	10418.51	887.75	20
H10B	3963.46	9962.73	1818.56	20
H11A	3726.06	10015.34	-701.85	20
H11B	3345.5	9644.29	-535.13	20
H12A	3484.52	9091.51	-1798.41	20
H12B	3950.36	9019.14	-1192.89	20
H14A	3898.41	8282.13	4180.07	37
H14B	3453.87	7973.73	3888.96	37
H14C	3517.13	8776.12	3885	37
H16A	3628.18	3978.1	5915.23	22
H16B	3614.5	4013.52	4805.15	22
H20A	3560.99	7125.1	6551.3	31
H20B	3840.66	6762.6	7512.35	31
H24A	3885.42	6294.46	3080.88	29
H24B	3655.3	6829.36	3554.11	29
H28A	2643.37	7811.37	4212.68	32
H28B	2264.95	7319.35	3809.09	32
H28C	2554.36	7470.75	3166.74	32
H17C	3638.07	5018.94	6826.19	20
H17D	4072.61	4697.69	6959.49	20
H18C	4109.48	5845.19	7542.42	22
H18D	4337.83	5743.29	6750.86	22
H21A	3889.24	7143.65	5510.49	22
H21B	4299.37	6945.27	6328.36	22
H22A	4309.82	6725.85	4685.56	24
H22B	4428.36	6080.06	5387.17	24
H25A	3818.14	5062.38	3742.32	21
H25B	4272.46	5333.77	4072.23	21
H26A	4178.98	4417.83	5072.52	23
H26B	4345.95	5088	5692.94	23
H17E	4337.71	5137.62	6116.85	22
H17F	4177.15	4544.76	6668.11	22
H18E	4212.91	5578.84	7501.09	22
H18F	3759.75	5309.08	7116.81	22
H21C	4405.04	6102.61	6298.6	24
H21D	4329.37	6856.53	6641.59	24
H22C	4314.3	6891.75	4968.88	21
H22D	3878.64	7081.84	5048.38	21
H25C	4372.75	5667.54	4979.24	22

H25D	4195.53	5605.6	3819.94	22
H26C	4143.53	4547.94	4622.57	22
H26D	3716.17	4808.86	3941.26	22
H18A	2272(7)	8947(18)	2310(30)	80
H17A	2379(7)	10776(17)	3340(30)	80
H18B	2667(11)	9103(19)	2890(30)	80
H17B	2650(11)	10269(19)	3750(30)	80
H19A	2529(6)	9215(18)	4390(30)	80
H19B	2948(10)	9039(17)	4915(19)	80

Atomic Occupancy for SOLUTION 1.

Atom	Occupancy	Atom	Occupancy	Atom	Occupancy
C17A	0.75	H17C	0.75	H17D	0.75
C18A	0.75	H18C	0.75	H18D	0.75
C21A	0.75	H21A	0.75	H21B	0.75
C22A	0.75	H22A	0.75	H22B	0.75
C25A	0.75	H25A	0.75	H25B	0.75
C26A	0.75	H26A	0.75	H26B	0.75
C17B	0.25	H17E	0.25	H17F	0.25
C18B	0.25	H18E	0.25	H18F	0.25
C21B	0.25	H21C	0.25	H21D	0.25
C22B	0.25	H22C	0.25	H22D	0.25
C25B	0.25	H25C	0.25	H25D	0.25
C26B	0.25	H26C	0.25	H26D	0.25

Table 9 Solvent masks information for final_BLS_05-13-22.

Number	X	Y	Z	Volume	Electron count	Content
1	0.000	-0.014	0.218	1206.1	409.440	water
2	0.500	-0.817	-0.763	1206.1	409.440	water

Refinement model description

Number of restraints - 4, number of constraints - unknown.

Details:

1. Fixed Uiso

At 1.2 times of:

All C(H,H) groups

At 1.5 times of:

All C(H,H,H) groups

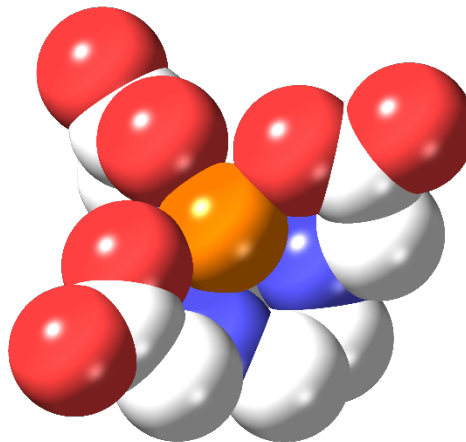
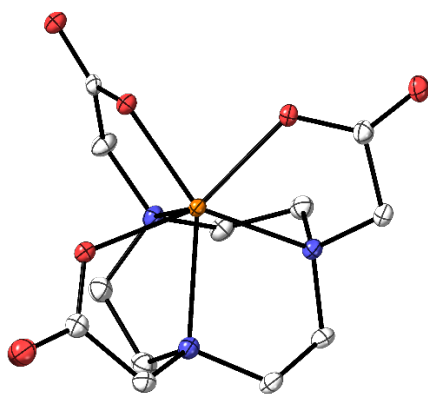
2. Restrained distances

H18A-O18

1 with sigma of 0.02

O17-H17A

1 with sigma of 0.02
 O19-H19A
 1 with sigma of 0.02
 H19B-O19
 0.95 with sigma of 0.02
 3. Uiso/Uaniso restraints and constraints
 Uanis(C18B) = Uanis(C17B)
 Uanis(C26B) = Uanis(C25B) = Uanis(C21A) = Uanis(C18B) = Uanis(C17B)
 4. Others
 Fixed Sof: C17A(0.75) H17C(0.75) H17D(0.75) C18A(0.75) H18C(0.75) H18D(0.75)
 C21A(0.75) H21A(0.75) H21B(0.75) C22A(0.75) H22A(0.75) H22B(0.75) C25A(0.75)
 H25A(0.75) H25B(0.75) C26A(0.75) H26A(0.75) H26B(0.75) C17B(0.25) H17E(0.25)
 H17F(0.25) C18B(0.25) H18E(0.25) H18F(0.25) C21B(0.25) H21C(0.25) H21D(0.25)
 C22B(0.25) H22C(0.25) H22D(0.25) C25B(0.25) H25C(0.25) H25D(0.25) C26B(0.25)
 H26C(0.25) H26D(0.25)
 Fixed Uiso: H18A(0.08) H17A(0.08) H18B(0.08) H17B(0.08) H19A(0.08) H19B(0.08)
 5.a Secondary CH2 refined with riding coordinates:
 C2(H2A,H2B), C3(H3A,H3B), C4(H4A,H4B), C6(H6A,H6B), C7(H7A,H7B), C8(H8A,H8B),
 C10(H10A,H10B), C11(H11A,H11B), C12(H12A,H12B), C16(H16A,H16B), C20(H20A,H20B),
 C24(H24A,H24B), C17A(H17C,H17D), C18A(H18C,H18D), C21A(H21A,H21B), C22A(H22A,
 H22B), C25A(H25A,H25B), C26A(H26A,H26B), C17B(H17E,H17F), C18B(H18E,H18F),
 C21B(H21C,H21D), C22B(H22C,H22D), C25B(H25C,H25D), C26B(H26C,H26D)
 5.b Idealised Me refined as rotating group:
 C14(H14A,H14B,H14C), C28(H28A,H28B,H28C)



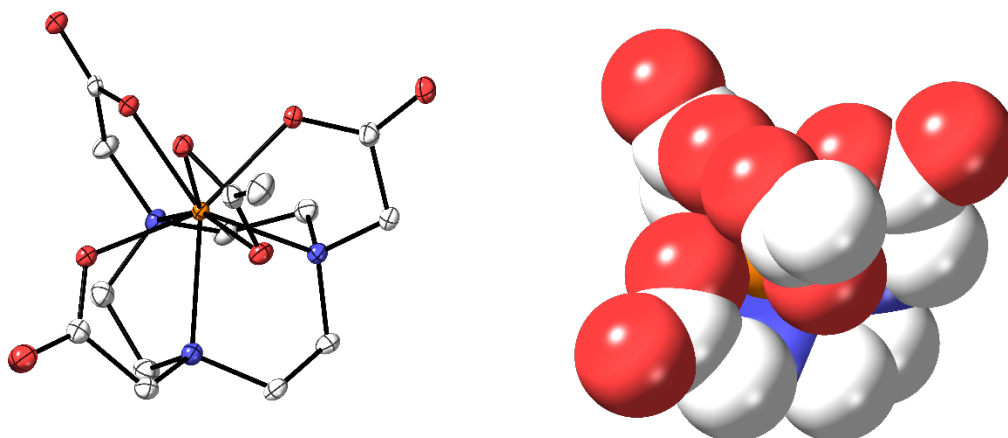


Figure S1. Molecular structure of Sc(NOTA) (top) and $[\text{Sc}(\text{NOTA})(\text{OOCCH}_3)]^{1-}$ (bottom). Spacefilling models of the structures (based on VanderWalls radii) are shown for comparison obtained from the single crystal X-ray data.

A discussion of the stereoelectronic coordination of the Sc^{3+} by NOTA^{3-} is provided in the text. Both a steric and electronic driving force seem to contribute to the coordination of the κ_2 - (OOCCH_3) . Above, the spacefilling model of the $[\text{Sc}(\text{NOTA})(\text{OOCCH}_3)]^{1-}$ fragment, both with and without the OOCCH_3^- displayed, shows the incomplete steric saturation provided by the hexadentate NOTA^{3-} fragment alone.

HRMS Analysis

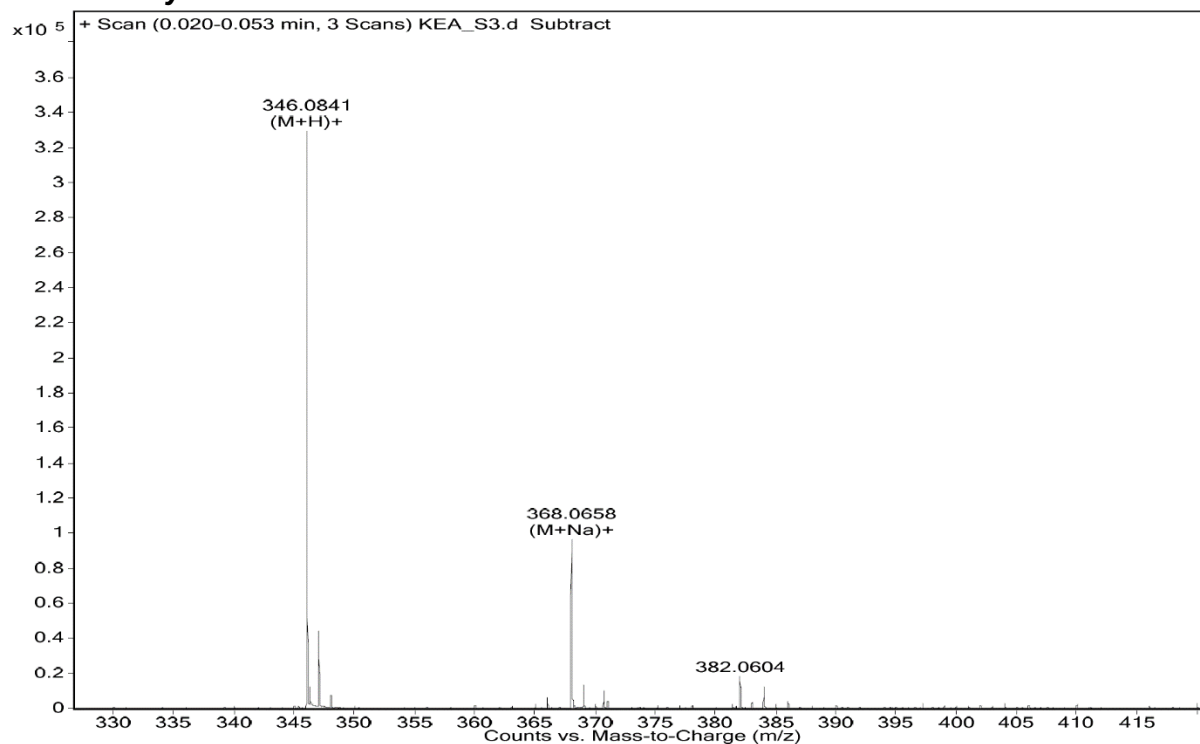


Figure S2. Mass Spectrum for Sc(NOTA) (ToF, positive mode).

MS Discussion

Observed by mass spec were two cations $[M+H]^+$ and $[M+Na]^+$. Here, $M = [Sc(NOTA)]$, the neutral chelated metal complex without the inclusion of a capping ligand. This observation is consistent with previous reports where a capping ligand is lost during ionization. Scanning in positive ion mode demonstrates the chelation of the NOTA macrocycle to the Sc^{3+} .

NMR Spectroscopy

General NMR Considerations

All NMR spectra were collected on a Bruker Avance 400 MHz spectrum or operating with a 5 mm broadband probe. ^1H NMR data was collected at 400.13 MHz in D_2O or $\text{dms}\text{-d}_6$ and referenced to the residual solvent peak as 4.79 ppm or 2.50 ppm respectively. ^{45}Sc NMR data was collected at 97.198 MHz, again in D_2O or $\text{dms}\text{-d}_6$. Chemical shifts were referenced to an external standard of $\text{Sc}(\text{NO}_3)_3$ (5 to 10 mg) dissolved in D_2O as 0 ppm. ^{17}O NMR was collected at 54.243 MHz and referenced to the ^{17}O NMR signal in tap water as 0 ppm. Samples were prepared using of $\text{Na}[\text{Sc}(\text{NOTA})(\text{OOCCH}_3)]$ (5 – 10 mg) dissolved in approximately 0.75 mL of solution. ^{45}Sc NMR acquisition parameters were as follows:

In D_2O

TD: 2048

d1: 0.1 sec

SW: 96153.8 hz

p1: 24.2 μS

pulse program: zgpg30

in $\text{dms}\text{-d}_6$

TD: 2048

d1: 0.5 sec

SW: 96153.8 hz

p1: 24.2 μS

pulse program: zgpg30

^1H and ^{17}O NMR acquisition parameters were unmodified from standard Bruker pulse sequences.

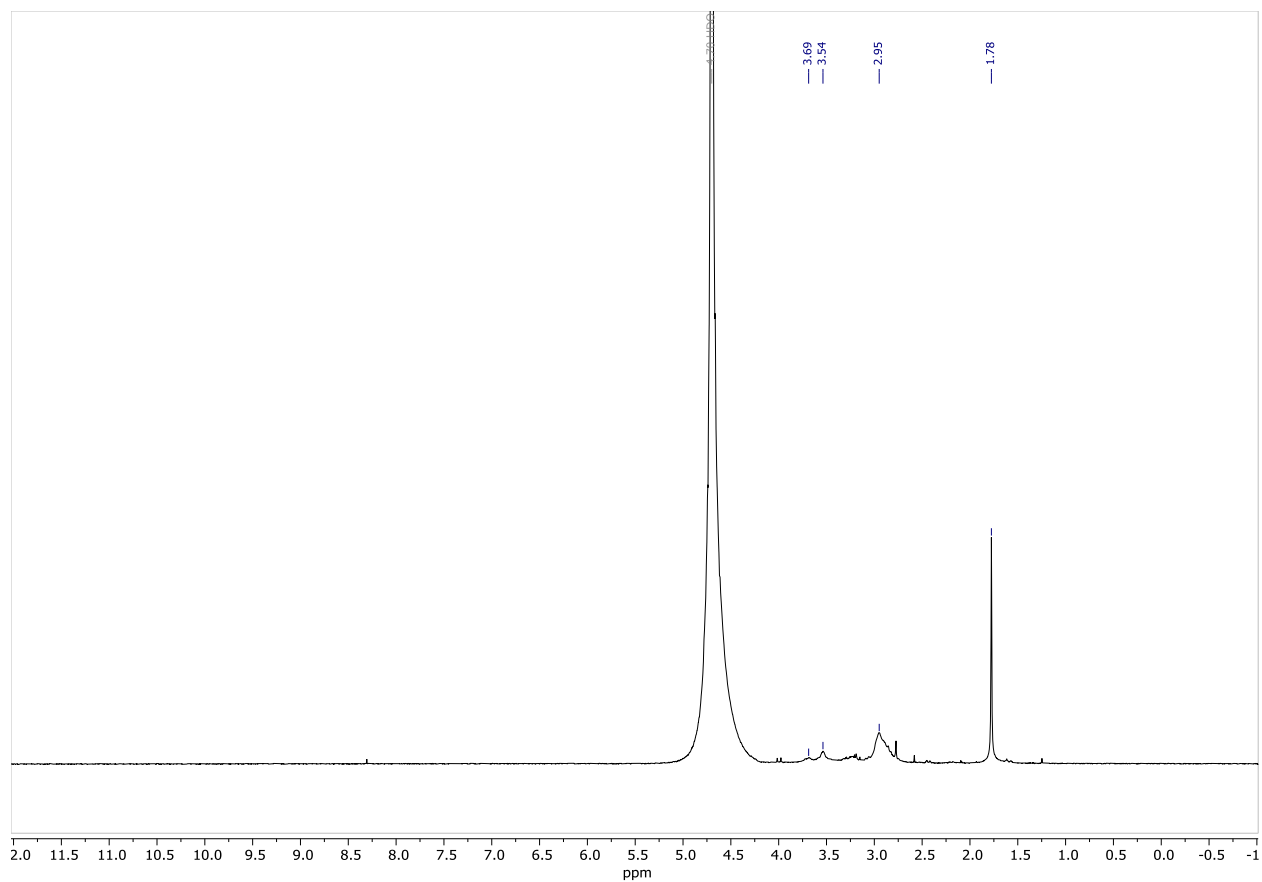


Figure S3. ^1H NMR of $\text{Na}[\text{Sc}(\text{NOTA})(\text{OOCCH}_3)]$ in D_2O at $20\text{ }^\circ\text{C}$ ($\text{pH} = 7$). Broad peaks indicative of an exchange process.

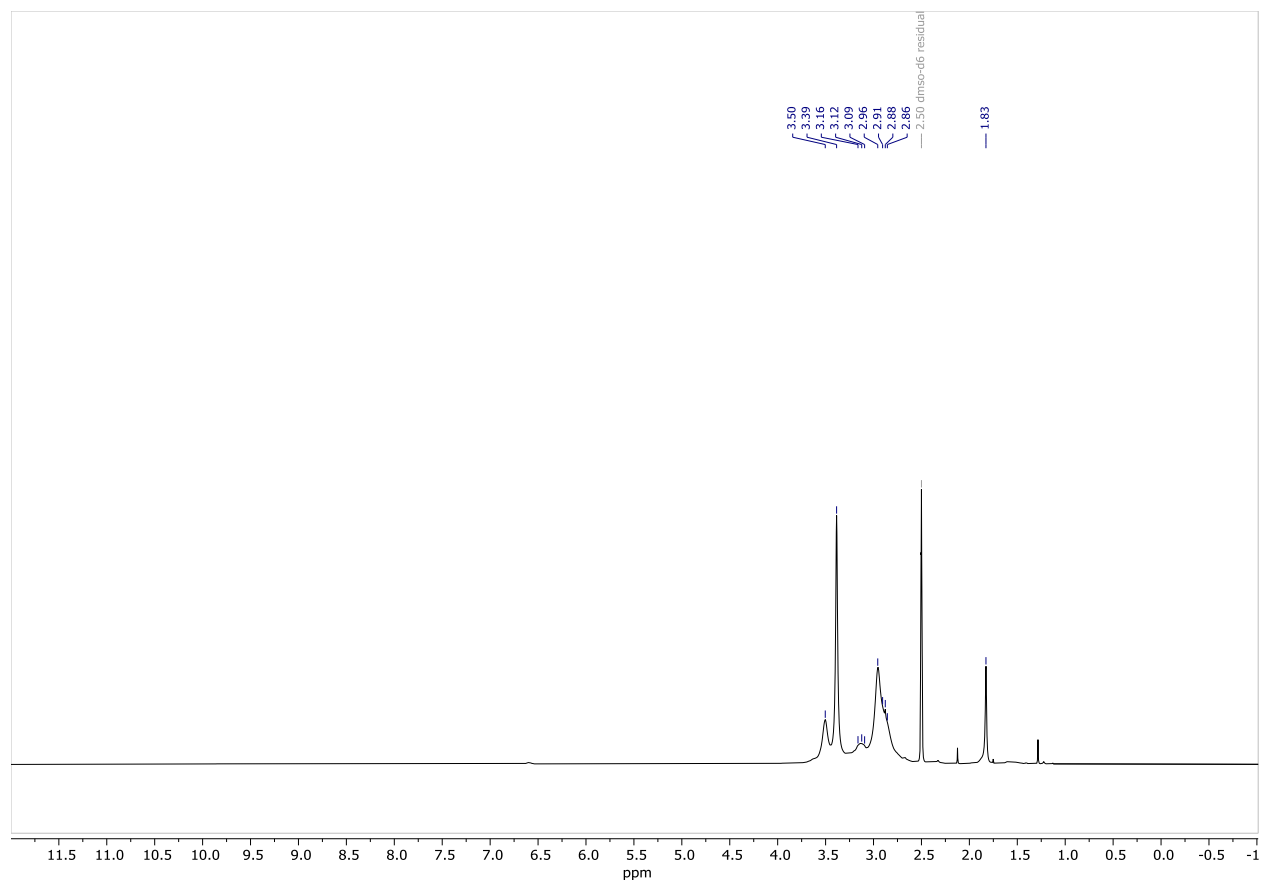


Figure S4. ^1H NMR of $\text{Na}[\text{Sc}(\text{NOTA})(\text{OOCCH}_3)]$ in $\text{DMSO-}d_6$ at $20\text{ }^\circ\text{C}$.

Note, in Figures S3 and 4 above, the broadness of the peaks indicates that there may be a dynamic structural rearrangement in solution. This could be due to isomeric shifts as has frequently been observed with +3 metal cations and the related ligand DOTA.⁴⁻⁷ In solution, such complexes can alternate between a square antiprismatic arrangement and a twisted square antiprismatic arrangement, where there is more or less alignment between the macrocyclic nitrogen and its respective acetate functional arm. This broadness precluded the observation of adequate signal to noise in ^{13}C NMR attempts with the sample concentrations utilized for additional ^{45}Sc NMR experiments.

Name: M1
From: 30.441 ppm
To: 155.000 ppm
Residual Error: 2.53e+12
ppmHeight Width(Hz)GArea
1 99.8237533518558 1.1905701567207
2 88.83590837439 0.9926929461968

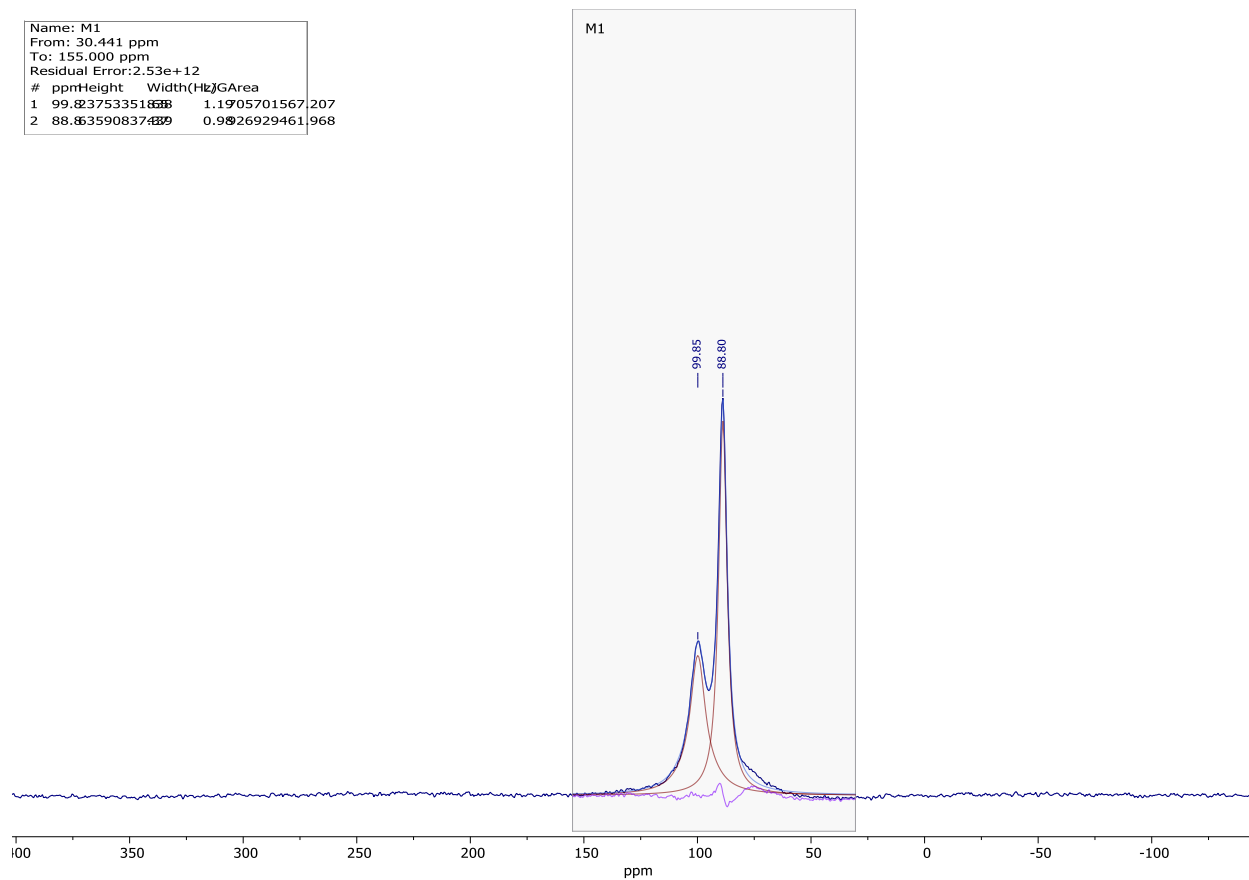


Figure S5. ^{45}Sc NMR of $\text{Na}[\text{Sc}(\text{NOTA})(\text{OOCCH}_3)]$ in D_2O at $20\text{ }^\circ\text{C}$.

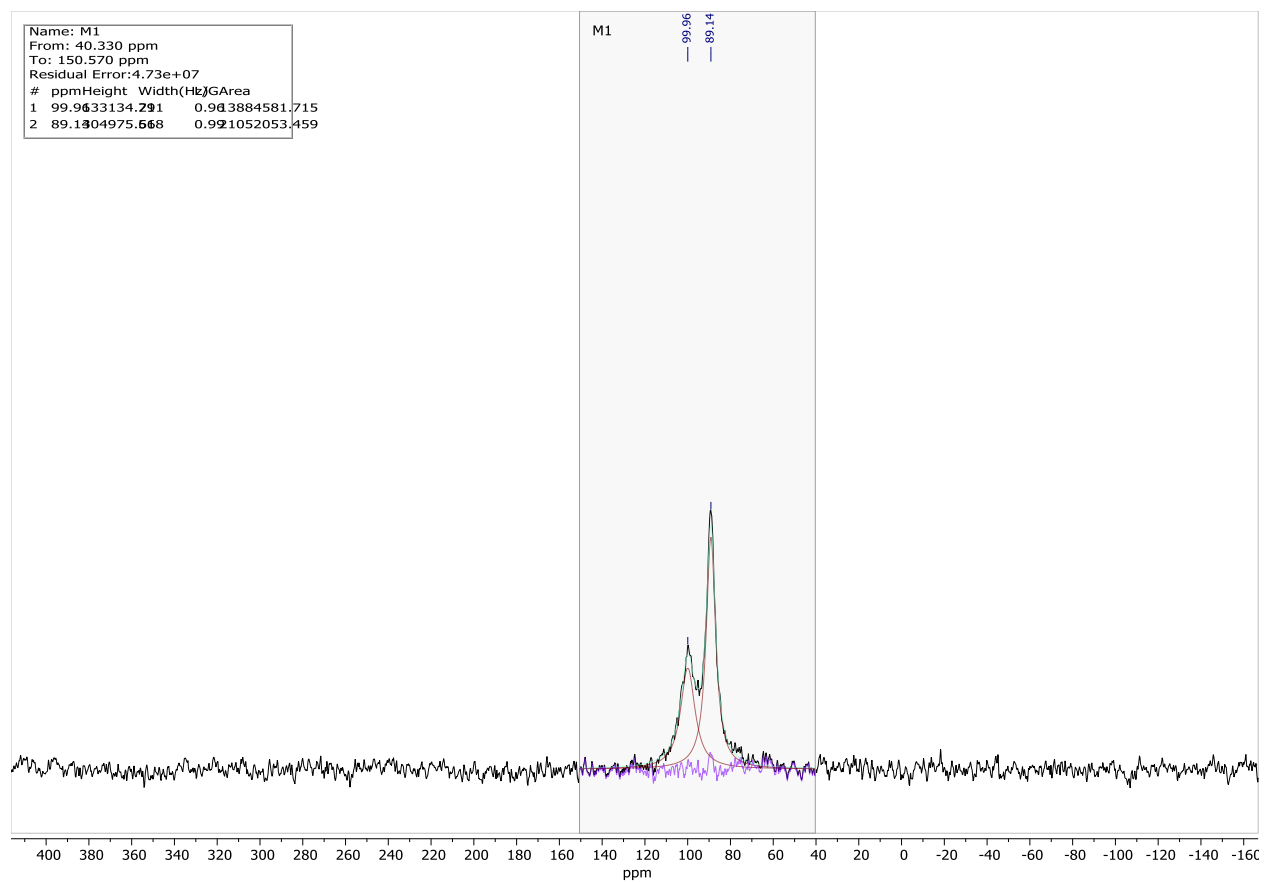


Figure S6. ^{45}Sc NMR of $\text{Na}[\text{Sc-NOTA-OAc}]$ in D_2O at $40\text{ }^\circ\text{C}$. Peak fitting was applied.

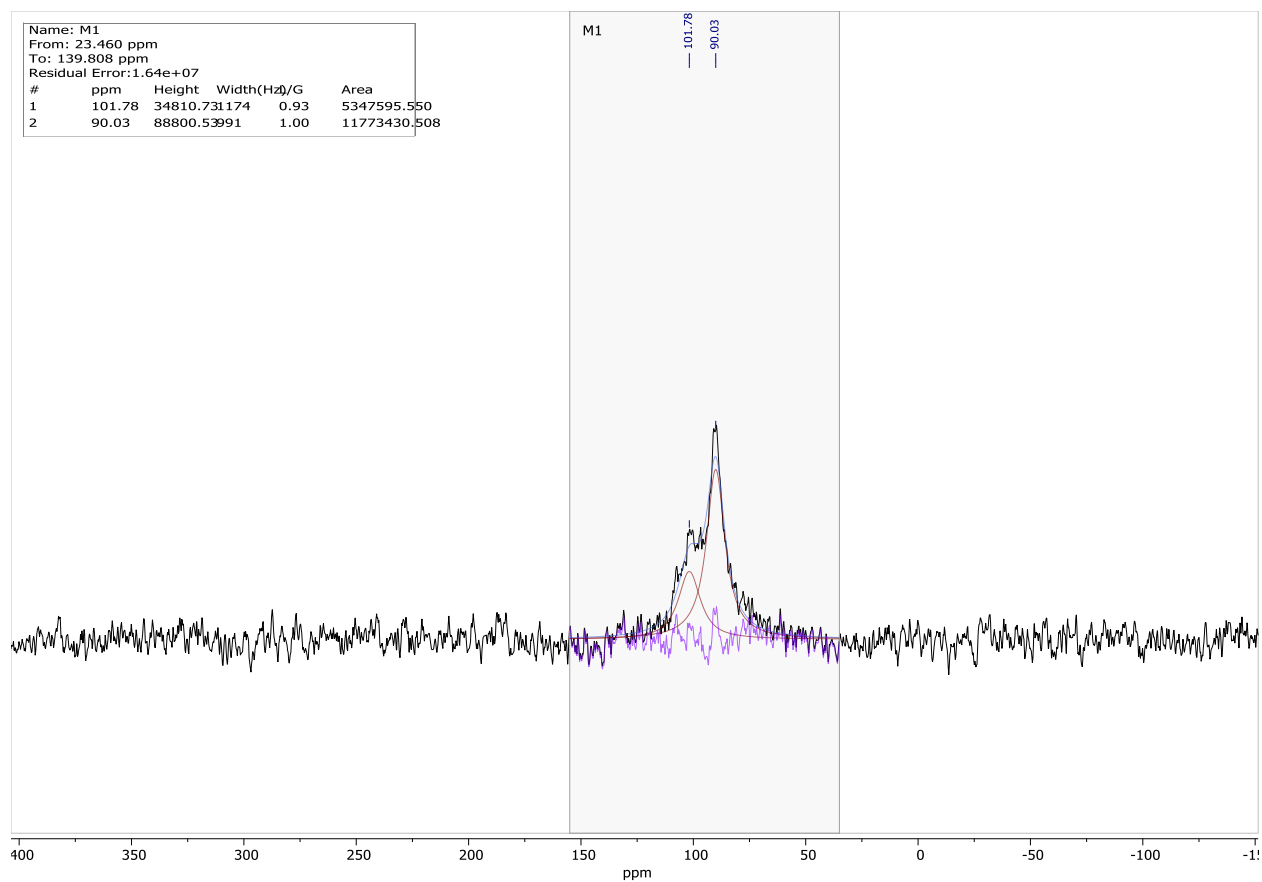


Figure S7. ^{45}Sc NMR of $\text{Na}[\text{Sc-NOTA-OAc}]$ in D_2O at $80\text{ }^\circ\text{C}$. Peak fitting was applied

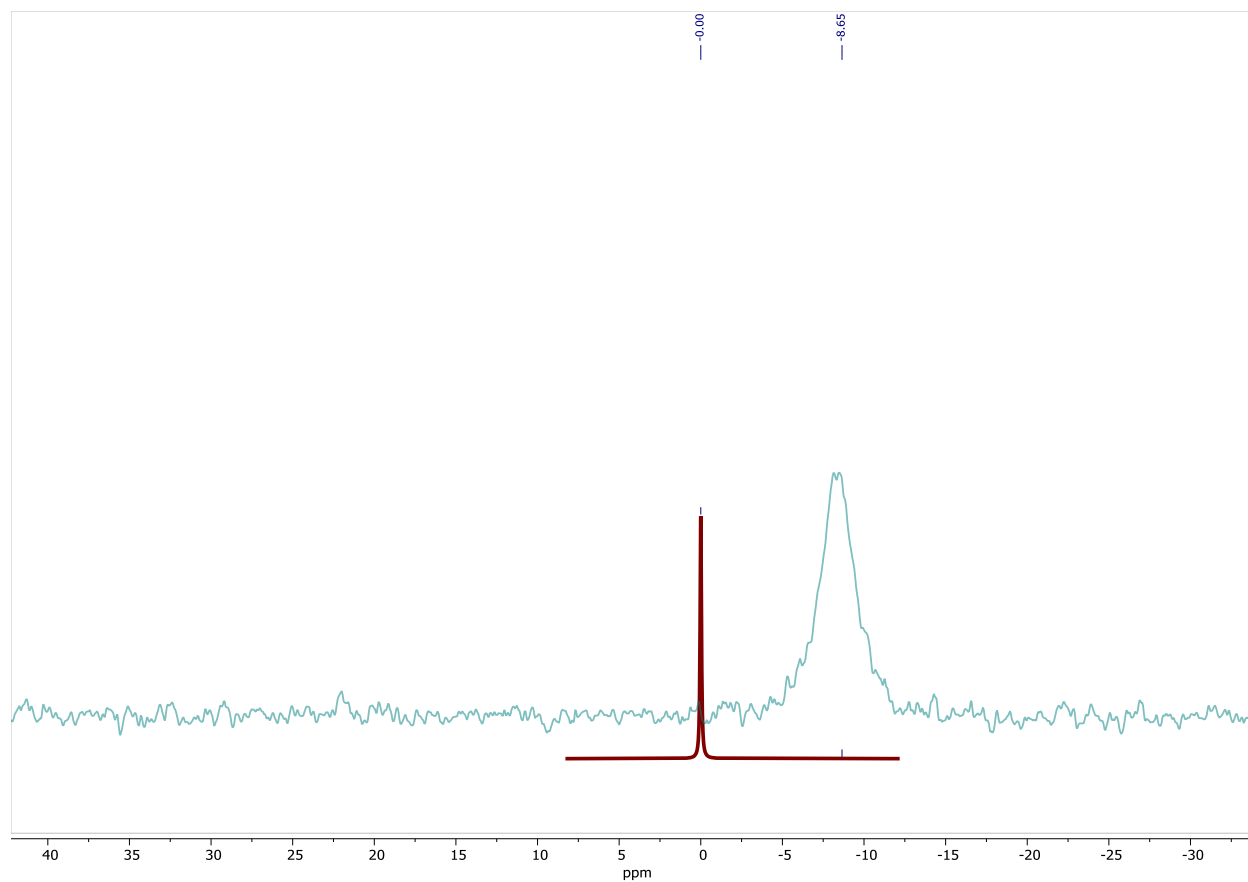


Figure S8. ^{17}O NMR spectra of tap water (red) and $\text{Na}[\text{Sc}(\text{NOTA})(\text{OOCCH}_3)]$ in D_2O spiked with $\text{H}_2(^{17}\text{O})$ (green) at 25 °C.

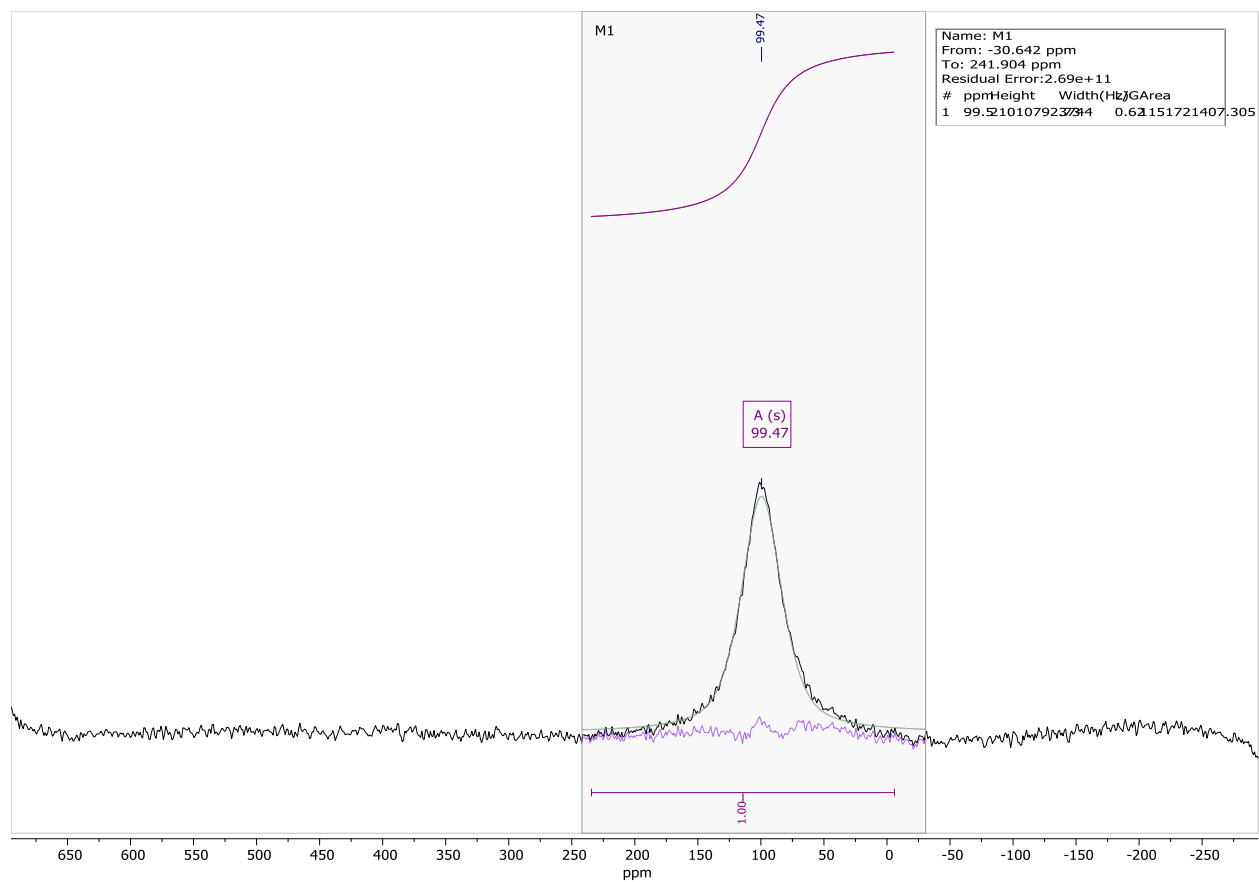


Figure S9. ^{45}Sc NMR of $\text{Na}[\text{Sc}(\text{NOTA})(\text{L})]$ in dms0-d_6 at $20\text{ }^\circ\text{C}$. (where $\text{L} = \text{OOCCH}_3$, DMSO , H_2O or a combination of these)

Experimental Approximation of Exchange Process Thermodynamics

Rearrangement of the Eyring equation, relating a reaction rate constant and the free energy of the reaction, leads to the Van't Hoff equation shown in Eq. 1 and reiterated here:

$$\ln(K_{eq}) = \frac{-\Delta H^\circ}{R} \cdot \left(\frac{1}{T}\right) + \frac{\Delta S^\circ}{R} \quad \text{Eq. S1}$$

Experimental determination of K_{eq} for a given equilibrium can be made at varying temperatures. Plotting $(1/T)$ as the x parameter, and $\ln(K_{eq})$ as the y parameter, it follows that $\Delta H^\circ = (-R \times \text{slope})$ and $\Delta S^\circ = (R \times \text{intercept})$ of the linear regression relating x and y . This approach was applied to the experimentally determined species distribution of **1** [Sc(NOTA)(OH₂)] and **2** (Na[Sc(NOTA)(OOCCH₃)]) by ⁴⁵Sc NMR spectroscopy at 3 different temperatures in D₂O.

We acknowledge that this approach assumes the peak areas are roughly proportional to the species concentrations in solutions, which would require similar quadrupole relaxation environments around the ⁴⁵Sc nuclei. Thus, we treat this exercise as an experimental approximation, rather than a strict, quantitative determination of the thermodynamics of the equilibrium process considered. Deconvolution of the overlapping ⁴⁵Sc NMR peaks was accomplished by analyzing the fourier transformed FID at each temperature using the peak fitting regime in MestreNova's software suite (V14.1.2). The results of these fits supplied the relative values given as "Area" and the calculated "% Area" in Table S4, below.

The NMR solution utilized for these experiments was prepared as follows: 18 mg of single-crystals (427 g/mol, 42 μmol) of Na[Sc(NOTA)(OOCCH₃)] were dissolved in 0.75 mL of D₂O to yield a solution that was ~0.056 M in [Sc-complex]. This concentration was used to calculate approximate *in situ* concentrations based on the area % found for the two species.

To clarify the assumptions made to reach the simplified equation for K_{eq} (Eq. 2), note that as water addition occurs to [Sc(NOTA)(OOCCH₃)]¹⁻, an equivalent amount of the hydrated product species, [Sc(NOTA)(OOCCH₃)(OH₂)]¹⁻, is generated. Thus, the total initial concentration of Sc(NOTA) complex added can be described as:

$$[Sc(NOTA)(OOCCH_3)^-]_i = [Sc(NOTA)(OOCCH_3)^-]_{eq} + [Sc(NOTA)(OOCCH_3)(OH_2)^-]_{eq} \quad \text{Eq. S2}$$

When treating the denominator of the K_{eq} equation (Eq. 2), the equilibrium occurs in water as the solvent. Therefore, if we approximate water as a pure liquid (~55.5 M, > 1000× more concentrated than any solutes), the activity is equal to 1 ([a_{H₂O}] = 1)), so it cancels out of the equation, leaving the simple relationship that:

$$K_{eq} \approx \frac{[Sc(NOTA)(OOCCH_3)(OH_2)^-]}{[Sc(NOTA)(OOCCH_3)^-]} \quad \text{Eq. S3}$$

Given that the two concentrations sum to the initial concentrations, their area% are proportional to their relative concentrations; thus $\ln(K_{eq})$ can be easily approximated from the NMR data.

Table S1. Van't Hoff plot parameters for VT ⁴⁵Sc NMR species distributions.

Temperature (°C)	Species No.	Shift (ppm)	Splitting (Hz)	Fitted Area	Area%	1/T (K ⁻¹)	Ln(K _{eq}) (calc'd)
20	1	99.9	4520	7.06E08	0.432	0.00341	-
	2	88.6		9.27E08	0.568		0.27269
40	1	99.96	4328	1.39E07	0.397	0.00319	-
	2	89.14		2.11E07	0.603		0.41622
80	1	101.78	4700	5.34E06	0.317	0.00283	-
	2	90.03		1.17E07	0.683		0.76843

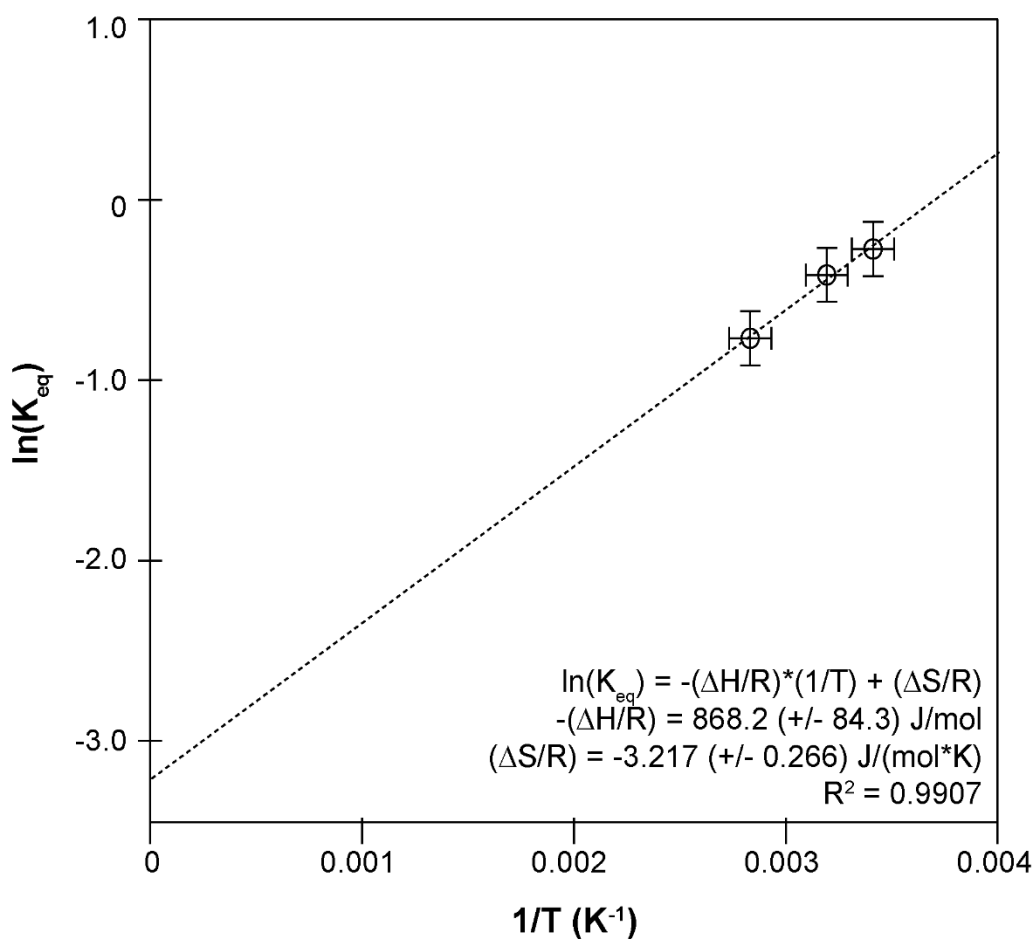


Figure S1. Van't Hoff Plot of VT ⁴⁵Sc NMR species distributions in D₂O (ln(K_{eq}) vs. (1/T))

The experimental data was plotted in IgorPro (9.0) and fitted with the standard linear regression included in the software package. The $R^2 = 0.9907$. Error estimates for T were converted for the x parameter based on an estimate of ± 5 °C probe calibration for temperature. The largest source of error estimated for K_{eq} is from the fitting error based on the curve separations to find Area and %

Area. The error is approximated at ~10% (a generous estimation from the residuals after curve fitting was applied in MestreNova).

IR Spectroscopy

IR spectroscopy was conducted using a commercial ThermoFisher Scientific Nicolet ID5 ATR-FTIR. Single crystals of the Na[Sc(NOTA)(OOCCH₃)] were dried briefly under vacuum and crushed to a powdery consistency. This solid material was deposited in a thin layer over the instrument window and directly measured as the pure solid.

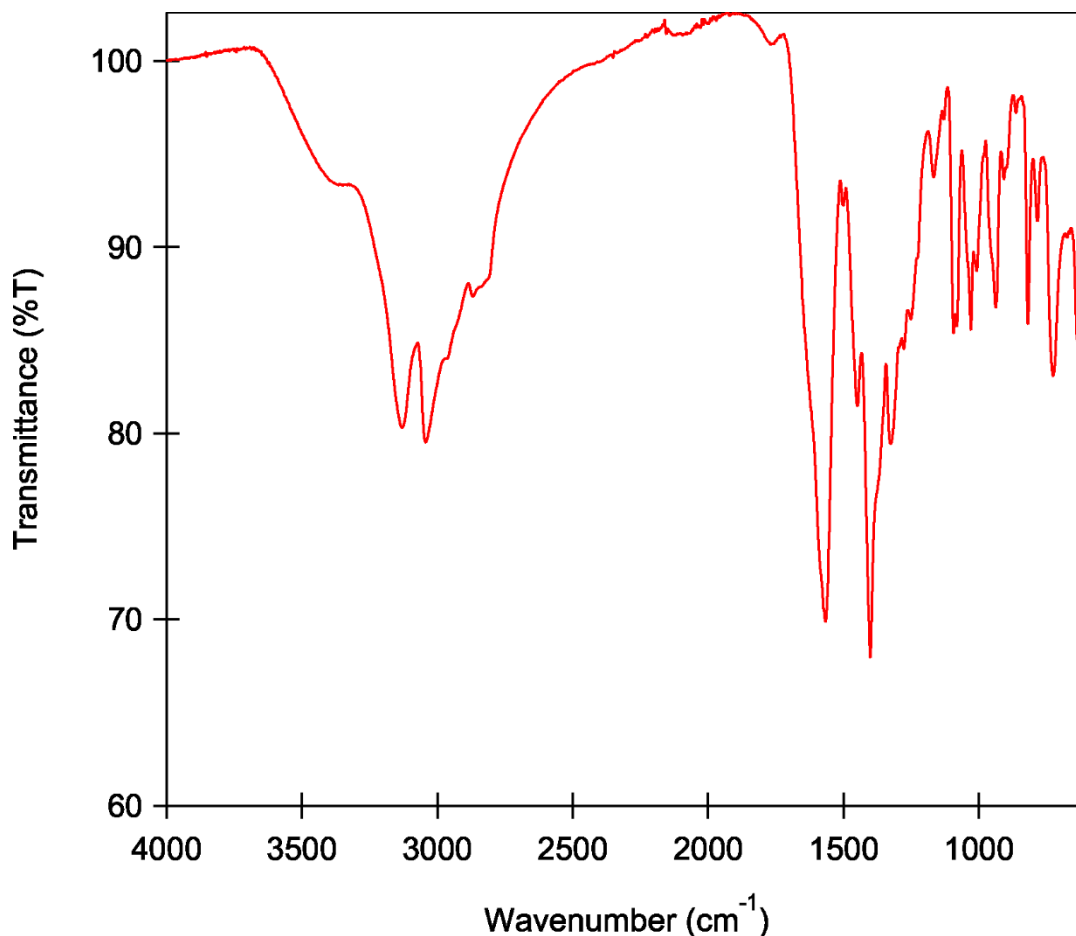


Figure S2. IR spectrum of solid Na[Sc(NOTA)(OOCCH₃)], recorded in transmittance mode.

Discussion of IR

The absorptive features observed in the IR spectrum of the solid sample agree well with the coordination environment observed for the complex in the single crystal X-ray structure. A variety of C–H stretches are observed in the region from 3300–2850 cm⁻¹. Also of note is the sharp feature

at 1570 cm^{-1} with a broad, sloping shoulder around 1630 . These absorptions correlate well with predicted C – O double bond stretches in the acetate arms. Likely a spread of energies occurs as different electrostatic contacts are observed in the solid state. Additionally, another strong absorption appears at 1400 cm^{-1} . This feature likely correlates to the acetate capping ligand C – O bonds. Finally, the fingerprint region has many sharp, but less intense features which we did not attempt to assign at length.

Computational Details

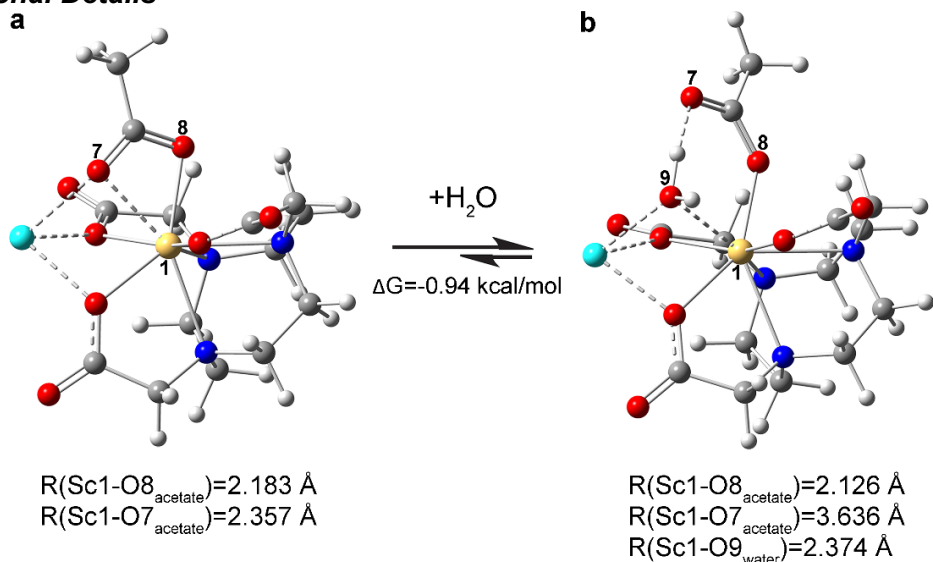
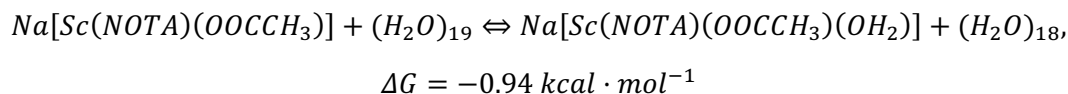
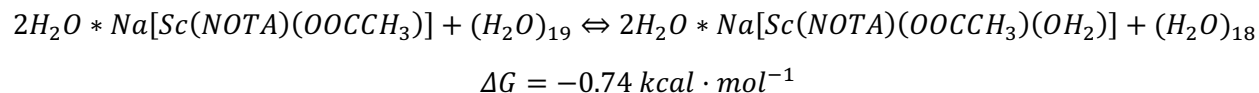


Figure S3. Coordination of water molecule to $\text{Na}[\text{Sc}(\text{NOTA})(\text{OOCCH}_3)]$ (a) to form $\text{Na}[\text{Sc}(\text{NOTA})(\text{OOCCH}_3)(\text{H}_2\text{O})]$ (b).

The considered water association is based on the following reaction:



Indeed, the Na ions are unlikely to be found undercoordinated in water solution. Accounting for the possible hydration of Na ions (1st coordination sphere) slightly changes the ΔG of this reaction:



the real solution, there could be more than one coordination sphere around the Na ion (2nd, 3rd, etc.) that could slightly affect the thermodynamics of the reaction due to the formation of additional hydrogen bonding interactions. However, the Na ions are expected to be similarly coordinated on the left and on the right side of the equations. So, to take advantage of the error cancellation effect (as the energies of reactions 2 and 3 are almost identical), we can employ unhydrated Na ions in our calculations, thus avoiding the necessity to account for all possible hydrogen bonding effects and excessive computational modeling of the hydration process including 2nd, 3rd, etc. coordination spheres for the $[\text{Sc}(\text{NOTA})(\text{OOCCH}_3)]^{1-}$ complex as well as for NaCH_3COO in the water-displacement reactions. Indeed, it is clear that the Na ions bound to the $[\text{Sc}(\text{NOTA})(\text{OOCCH}_3)]^{1-}$ are expected to be hydrated in the real water solution, but the use of the bare Na ions does not change the thermodynamics of the calculations in any appreciable way and thus can be employed here to save computational time. For consistency, a similar approach is further used for the acetate-water substitution reactions (described below) as well as for the possible association/substitution reactions of the $[\text{Sc}(\text{NOTA})(\text{OOCCH}_3)]^{1-}$ complex with DMSO.

As one can see from Table below, including Na ion (both bare or hydrated Na⁺) helps to describe the structure of the [Sc(NOTA)(OOCCH₃)]¹⁻ complex more accurately than excluding it. Presence of the Na ion decreases RMSD value (on all atoms) thus showing smaller deviations of the calculated structures from the experimental crystal structure.

Table S5. Comparison of the bond distances and RMSD values of the [Sc(NOTA)(OOCCH₃)]¹⁻, Na[Sc(NOTA)(OOCCH₃)] and 2H₂O*Na[Sc(NOTA)(OOCCH₃)] complexes to the experimental XRD structure.

Sc-NOTA	Sc-L	Exp.	Theor.	Theor.	Theor.
			[Sc(NOTA)(OOCCH ₃)]	Na[Sc(NOTA)(OOCCH ₃)]	2H ₂ O*Na[Sc(NOTA)(OOCCH ₃)]
	Sc – O _{NOTA} (Avg., Å)	2.148 (0.019)	2.132	2.136	2.133
	Sc – N _{NOTA} (Avg., Å)	2.390 (0.024)	2.467	2.423	2.427
Sc–OOCCH ₃	Sc – O _{OOCCH₃} (1) (Avg., Å)	2.197 (0.023)	2.195	2.183	2.180
	Sc – O _{OOCCH₃} (2) (Avg., Å)	2.352(0.035)	2.322	2.357	2.342
	RMSD from exp, Å		0.251	0.206	0.165

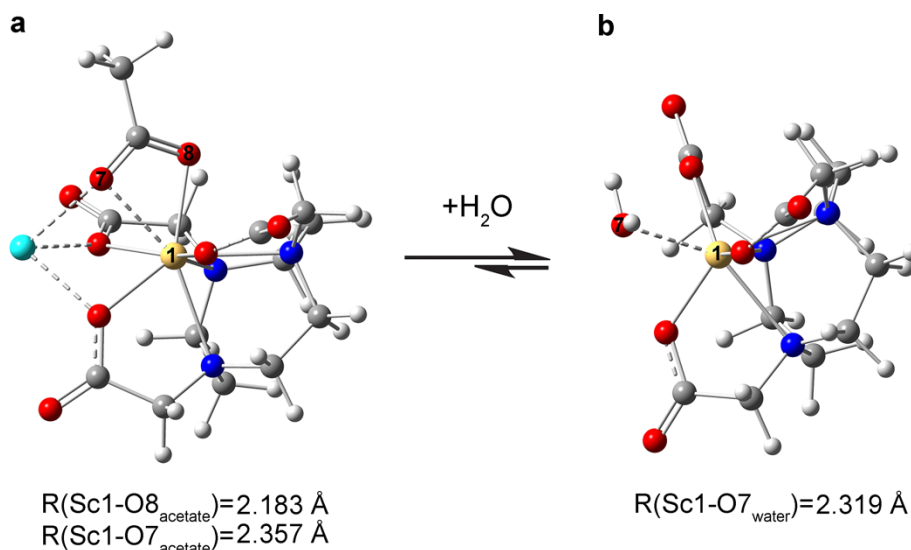
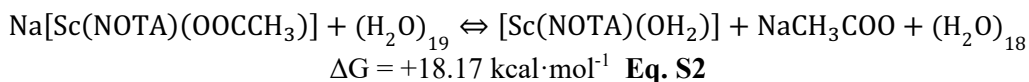


Figure S4. Acetate-water substitution in the Na[Sc(NOTA)(OOCCH₃)] complex (a) to form [Sc(NOTA)(OH₂)] (b).



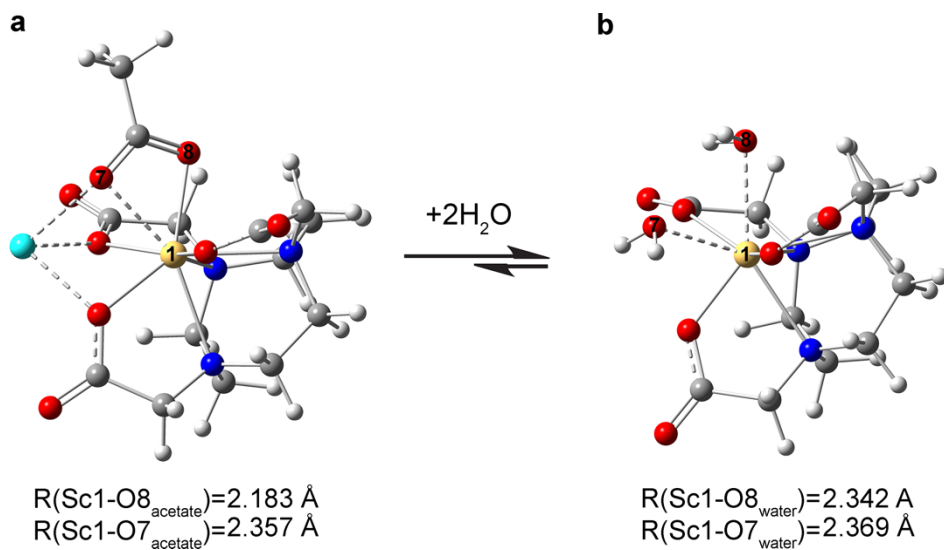
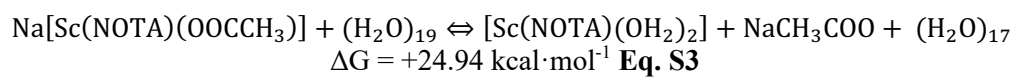
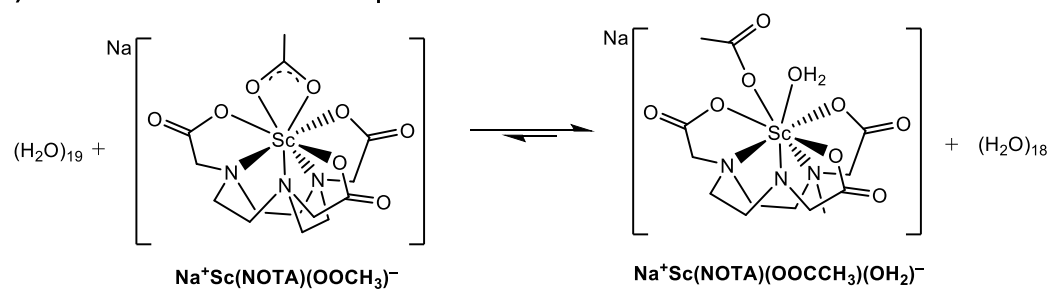


Figure S5. Acetate-water substitution with two water molecules to the $\text{Na}[\text{Sc}(\text{NOTA})(\text{OOCCH}_3)]$ complex (a) to form $[\text{Sc}(\text{NOTA})(\text{OH}_2)_2]$ (b).

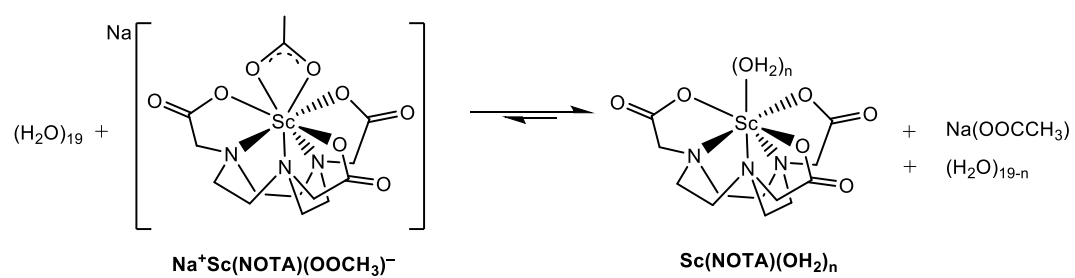


a) Water-Association with γ -Acetate



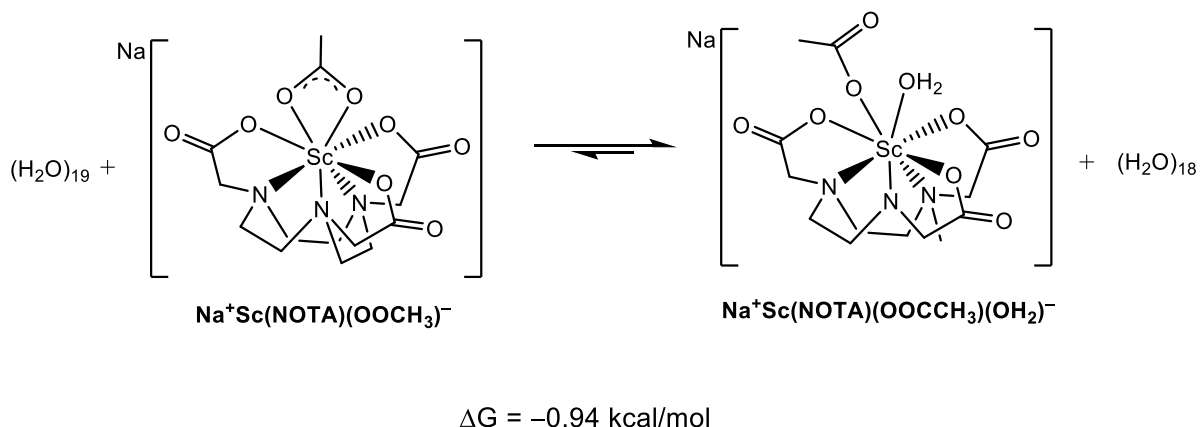
$$\Delta G = -0.94 \text{ kcal/mol}$$

b) Water-Acetate Exchange



$$\Delta G = 18.17 \text{ (n = 1) or } 24.94 \text{ (n = 2) kcal/mol}$$

a) Water-Association with 1 -Acetate



b) Water-Acetate Exchange

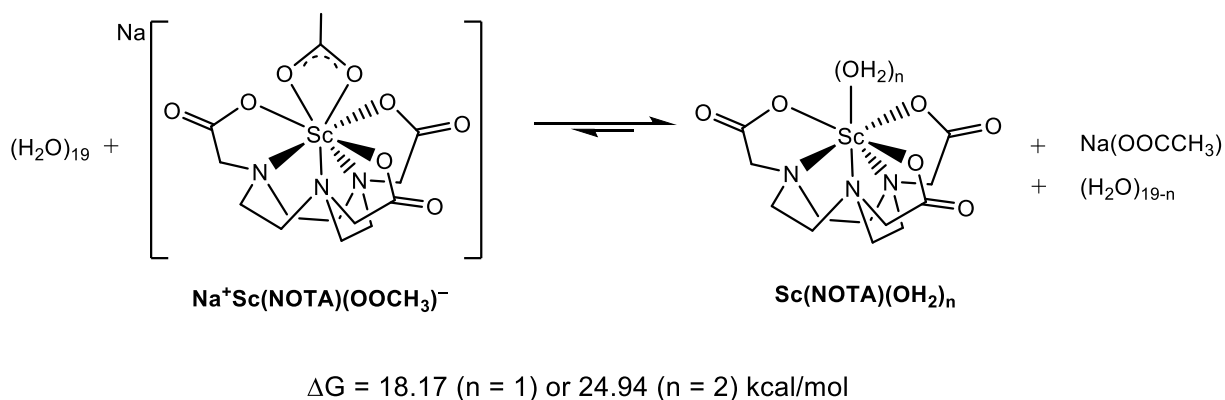
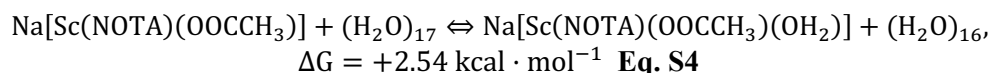


Figure S6. Exchange processes calculated and associated Gibbs free energy change for both the association (a) and exchange mechanisms (b).

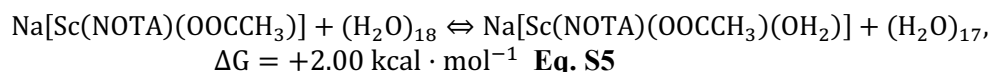
Discussion of Bulk Water Treatment Using the Cluster Approach

Coordination of water molecule to $\text{Na}[\text{Sc}(\text{NOTA})(\text{OOCCH}_3)]$ was considered using four approaches (a-d) based on the global minimum structures of water clusters previously determined in gas-phase calculations.⁸ Note, in each case, the structures of the $(\text{H}_2\text{O})_n$ and $(\text{H}_2\text{O})_{n+1}$ clusters were fully optimized in a water continuum using the PCM model:

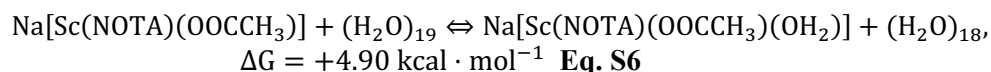
a) Using the $(\text{H}_2\text{O})_{17}$ cluster on the left side of the equation, and $(\text{H}_2\text{O})_{16}$ on its right side:



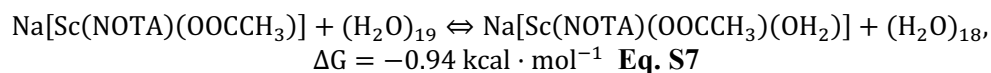
b) Using the $(\text{H}_2\text{O})_{18}$ cluster on the left side of the equation, and $(\text{H}_2\text{O})_{17}$ on its right side:



c) Using the (H₂O)₁₉ cluster on the left side of the equation, and (H₂O)₁₈ on its right side:



d) Using the (H₂O)₁₉ cluster on the left side of the equation, and (H₂O)₁₈ on its right side. The geometry of the (H₂O)₁₈ cluster was fully optimized in the water medium in PCM. (H₂O)₁₉ was modeled by adding one water molecule to (H₂O)₁₈ and optimizing it to its local minimum.



As shown previously, a large structural rearrangement occurs from the global minimum (H₂O)₁₈ (Pr44244) to the (H₂O)₁₉ (globular) cluster in gas phase.⁸ In order to minimize the reorganization energy associated with this rearrangement, we considered the (H₂O)₁₈ cluster optimized in water PCM as the representative of bulk water due to its similarity to the other water clusters, while the (H₂O)₁₉ cluster was obtained by adding one water molecule to (H₂O)₁₈ and optimizing it to the local minimum in the water medium in PCM. Please note that these water clusters may not necessarily represent their global minima configurations in the water since their structures were initially determined from the gas-phase calculations and only a local minimization was applied in PCM.⁸ Generally, with the increase of the cluster size, the solvation energy of water clusters gets closer to the bulk configuration and its energy. In the bulk, the hydrogen bonding network will not change much with one water molecule more or less. We think that the approach (d) describes the hydration process more accurately due to the significantly smaller structural rearrangement between the (H₂O)₁₈ and the new (H₂O)₁₉ water clusters.

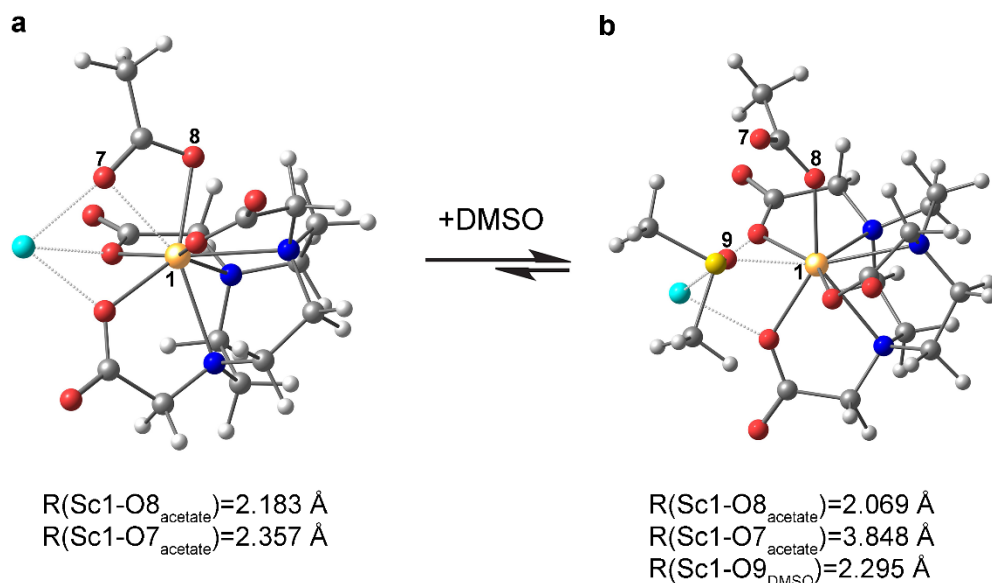
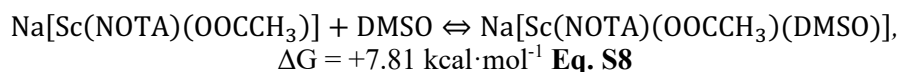


Figure S16. Coordination of DMSO molecule to Na[Sc(NOTA)(OOCCH₃)].



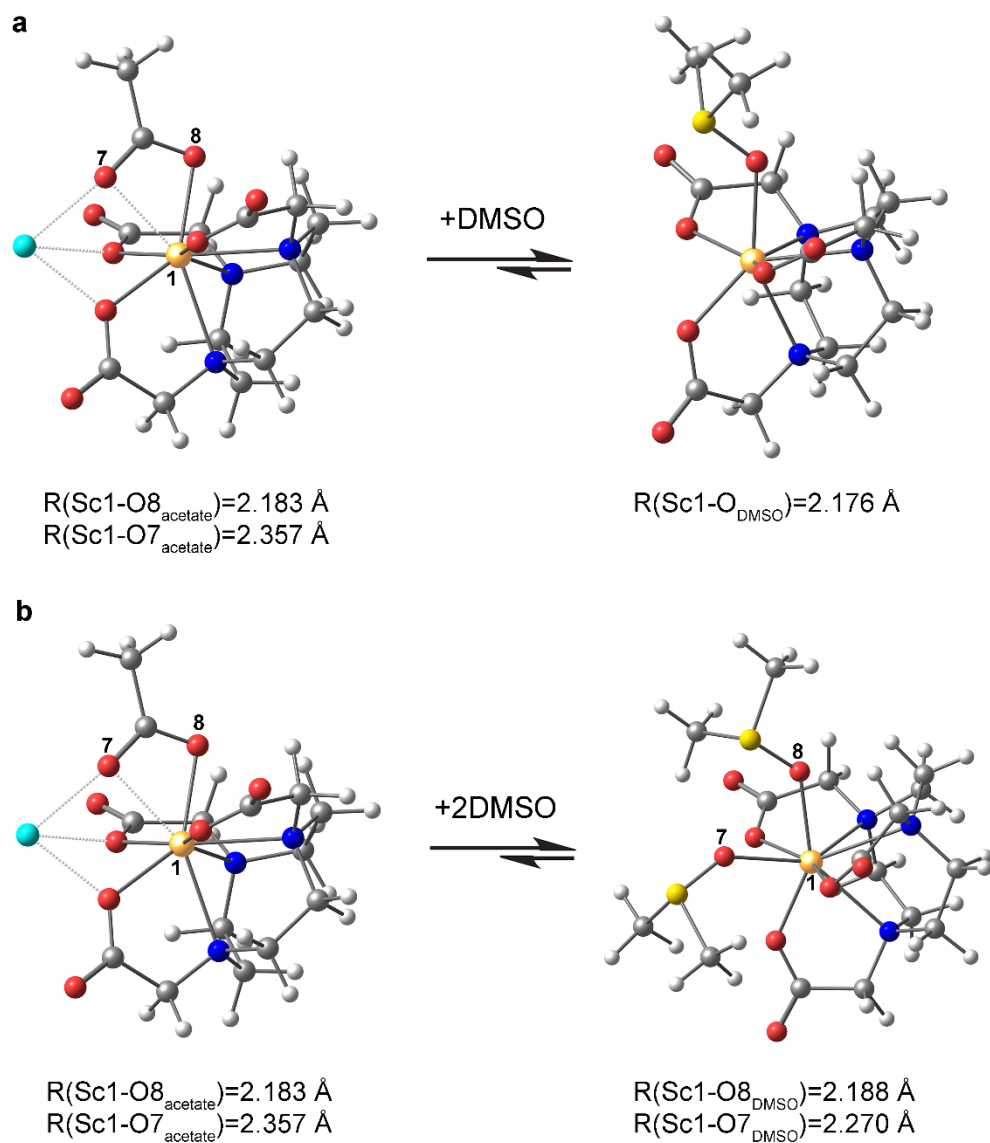
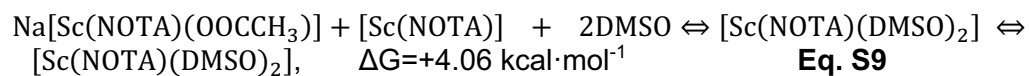
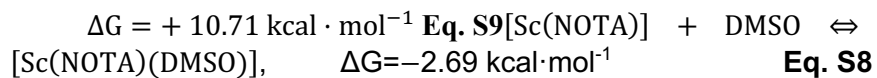


Figure S77. Acetate-DMSO substitution with one (**a**) and two (**b**) DMSO molecules in the $\text{Na}[\text{Sc}(\text{NOTA})(\text{OOCCH}_3)]$ complex to form $[\text{Sc}(\text{NOTA})(\text{DMSO})]$ (**a**) and $[\text{Sc}(\text{NOTA})(\text{DMSO})_2]$ (**b**)



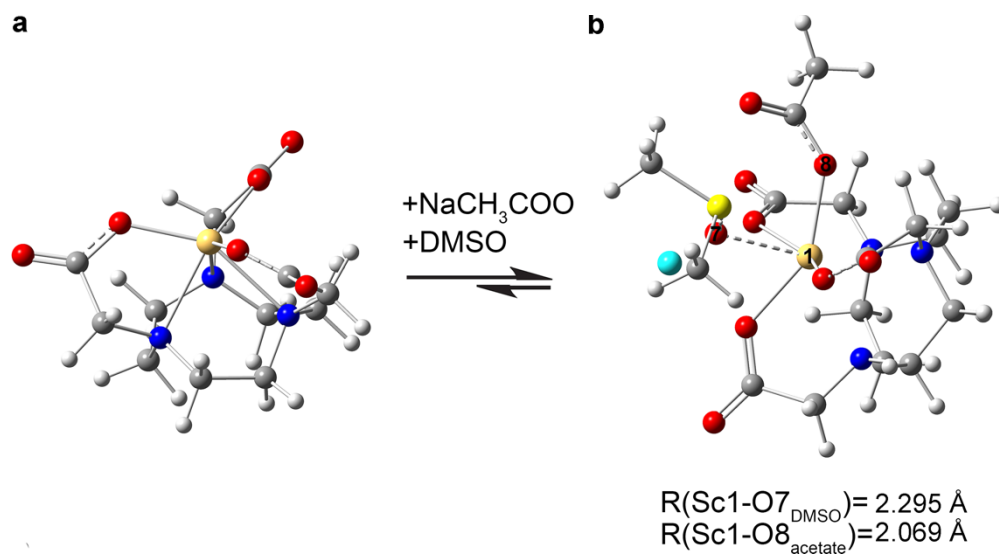
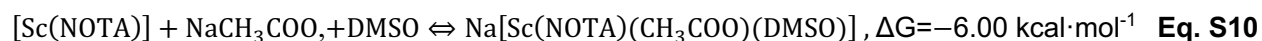


Figure S88. Simultaneous addition of DMSO and NaCH₃COO to [Sc(NOTA)] (a) to form Na[Sc(NOTA)(CH₃COO)(DMSO)] (b).



References

- 1 O. V. Dolomanov, L. J. Bourhis, R. J. Gildea, J. A. K. Howard and H. Puschmann, *J. Appl. Crystallogr.*, 2009, **42**, 339–341.
- 2 G. M. Sheldrick, University of Gottingen, Germany, 2016
- 3 A. L. Spek, *Acta Crystallogr. Sect. C Struct. Chem.*, 2015, **71**, 9–18.
- 4 K. J. Miller, A. A. Saherwala, B. C. Webber, Y. Wu, A. D. Sherry and M. Woods, *Inorg. Chem.*, 2010, **49**, 8662–8664.
- 5 C. Kumas, W. S. Fernando, P. Zhao, M. Regueiro-Figueroa, G. E. Kiefer, A. F. Martins, C. Platas-Iglesias and A. D. Sherry, *Inorg. Chem.*, 2016, **55**, 9297–9305.
- 6 J. Blahut, P. Hermann, Z. Tošner and C. Platas-Iglesias, *Phys. Chem. Chem. Phys.*, 2017, **19**, 26662–26671.
- 7 F. Benetollo, G. Bombieri, L. Calabi, S. Aime and M. Botta, *Inorg. Chem.*, 2003, **42**, 148–157.4
- 8 J. T. Su, X. Xu and W. A. G. Iii, 2004, 10518–10526.